Downstream Effects of the Pelton-Round Butte Hydroelectric Project on Bedload Transport, Channel Morphology, and Channel-Bed Texture, Lower Deschutes River, Oregon

Heidi Fassnacht[1] and Ellen M. McClure[2]

Oregon State University, Dept. of Geosciences and Dept. of Civil, Construction, and Environmental, and Engineering, Corvallis, Oregon

Gordon E. Grant

U.S. Forest Service, Pacific Northwest Research Station, Corvallis, Oregon

Peter C. Klingeman

Oregon State University, Department of Civil, Construction, and Environmental Engineering, Corvallis, Oregon

Field, laboratory, and historical data provide the basis for interpreting the effects of the Pelton-Round Butte dam complex on the surface water hydrology and geomorphology of the lower Deschutes River, Oregon, USA. The river's response to upstream impoundment and flow regulation is evaluated in terms of changes in predicted bedload transport rates, channel morphology, and channel-bed texture. Using a hydraulic model, we predicted discharges between 270 and 460 m^3/s would be required to initiate bedload transport. Analysis of morphologic change at a long-term cross-section showed general scour and fill beginning at approximately 250 m^3/s. Such bed-mobilizing flows have occurred less than 1% of the time during the 70+-year period of record, substantially less frequently than on other alluvial rivers. Historical streamflow records and bedload transport modeling suggest dam operations have had only minimal effects on the frequency and magnitude of streamflow and bedload transport. Analysis of gage data collected just below the dam complex revealed slow, minor degradation of the channel over the entire period of record, indicating the dams have not noticeably accelerated long-term incision rates. The dams also have had only minimal effect on channel-bed texture, as demonstrated by detailed analysis of longitudinal trends in surface and subsurface grain-sizes and bed armoring. This study presents a coherent story of the Deschutes River as a stable alluvial system. This stability appears to be due to a hydrologically uniform flow regime and low rates of sediment supply, neither of which has been substantially altered by the dams or their operation.

INTRODUCTION

Dams alter the movement of water, sediment, wood, and organisms through rivers and can, therefore, have potentially significant effects on alluvial systems. Predicting the magnitude, timing, extent, or duration of dam effects is complex, however [e.g., *Petts*, 1979, 1980; *Williams and*

[1]Currently at U.S. Peace Corps, Senegal, West Africa.

[2]Currently at Biohabitats, Inc., Timonium, Maryland.

Geology and Geomorphology of the Deschutes River, Oregon
Water Science and Application 7

10/1029/007WS12

Wolman, 1984]. Physical changes to channels downstream of dams can range from bed degradation and narrowing, to changes in channel-bed texture or armoring, to bed aggradation, bar construction, and channel widening, to no measurable change whatsoever [*Petts*, 1979; *Williams and Wolman*, 1984; *Chien*, 1985; *Galay et al.*, 1985; *Gilvear and Winterbottom*, 1992; *Collier et al.*, 1996]. The variability in channel responses downstream of dams reflects the complex interplay between the degree of flow regime alteration, the frequency of flows capable of transporting sediment, and the rate at which new sediment is supplied to the channel relative to the amount trapped by the dam [*Williams and Wolman*, 1984; *Grant and Schmidt*, this volume]. These complex and interacting factors limit our ability to predict the effect of any given dam on the downstream channel. Field and modeling studies are typically required to evaluate downstream changes and relate them directly to a dam and its operation. Such studies are becoming increasingly important as the operating rules and licenses for both Federal and non-Federal dams are renewed, and in light of changing societal expectations and objectives for river management.

This paper examines the downstream effects of the Pelton-Round Butte Hydroelectric Project (hereafter the "Project") on the lower Deschutes River in north-central Oregon (Figure 1). We report and synthesize the results of coordinated studies. Major individual components include a bedload transport study to estimate frequency and magnitude of streamflow and bedload transport prior to and following Project construction [*Fassnacht*, 1998]; a channel morphology study to identify temporal trends and magnitudes of changes in channel cross-section; and a channel-bed texture study to evaluate longitudinal trends in bed-material properties downstream of the Project [*McClure*, 1998]. Results from the channel morphology study complement those from *Curran and O'Connor* [this volume]. Observed responses of the Deschutes River are interpreted in light of the geologic and geomorphic setting of the river.

In the bedload transport study, the percentage of time that threshold transport conditions were equaled or exceeded was calculated based on field data, hydraulic modeling, and analysis of historical streamflow records. The robustness of the modeling results was confirmed by a sensitivity analysis and a detailed analysis of long-term cross-section change in relation to discharge. These results suggested extremely low bedload transport rates that would be difficult to measure directly in the field. To estimate the frequency and magnitude of bedload transport prior to and following Project construction, bedload transport modeling was conducted and evaluated in the context of historical streamflow records.

Although we did not calculate a sediment budget, repeat surveys of Project reservoirs provided first-order estimates of pre-dam sediment supply to the lower river. In addition, field observations were used to assess relative inputs of bed material from tributaries during high flow events.

Effects of the Project on downstream channel morphology and channel-bed texture were examined by using historical cross-sections to measure channel aggradation or scour and using a field program designed to evaluate changes in the grain-size distribution of the channel bed. No pre-dam grain-size measurements exist for the lower Deschutes River. Prior post-dam studies [*Huntington*, 1985] did not retain all particle sizes for measurement, precluding comparison of current particle-size distributions with previous particle-size measurements. It was not possible to obtain representative samples of bed material upstream of the Project due to the location of major tributary confluences and associated fans, and to the large area inundated by the reservoir created by the Project. Consequently, we substituted space for time and examined downstream longitudinal trends in the size of the surface and subsurface bed-material to evaluate the magnitude and extent of channel response. In addition, due to a large flood event that occurred after our first field season, we were also able to evaluate channel response by examining these same longitudinal trends prior to and following a large flood. Taken together, these different lines of evidence present a coherent and consistent story of the Deschutes River and Project effects.

STUDY AREA

The study area is located in the 27,200 km^2 Deschutes River basin in north-central Oregon (Figure 1). The Project (FERC No. 2030), a three-dam hydroelectric complex on the mainstem Deschutes River, is located directly downstream from the confluence of the Crooked, upper Deschutes, and Metolius Rivers (Figure 1). The Project includes Round Butte Dam, at River Mile[1] (RM) 110.1, Pelton Dam (RM 102.6), and the Reregulating Dam (RM 100.1). The study area encompassed the downstream-most 161 km of river extending from the Reregulating Dam to the confluence of the Deschutes and Columbia Rivers (Figure 1). Within this

[1] Units given are metric except for locations, which are given as River Miles (RM), or miles upstream from the river mouth as marked on USGS topographic maps. These values are close to, but not necessarily the same as, actual distances along the present channel. Fractional river miles given herein are based on interpolations between these published river miles.

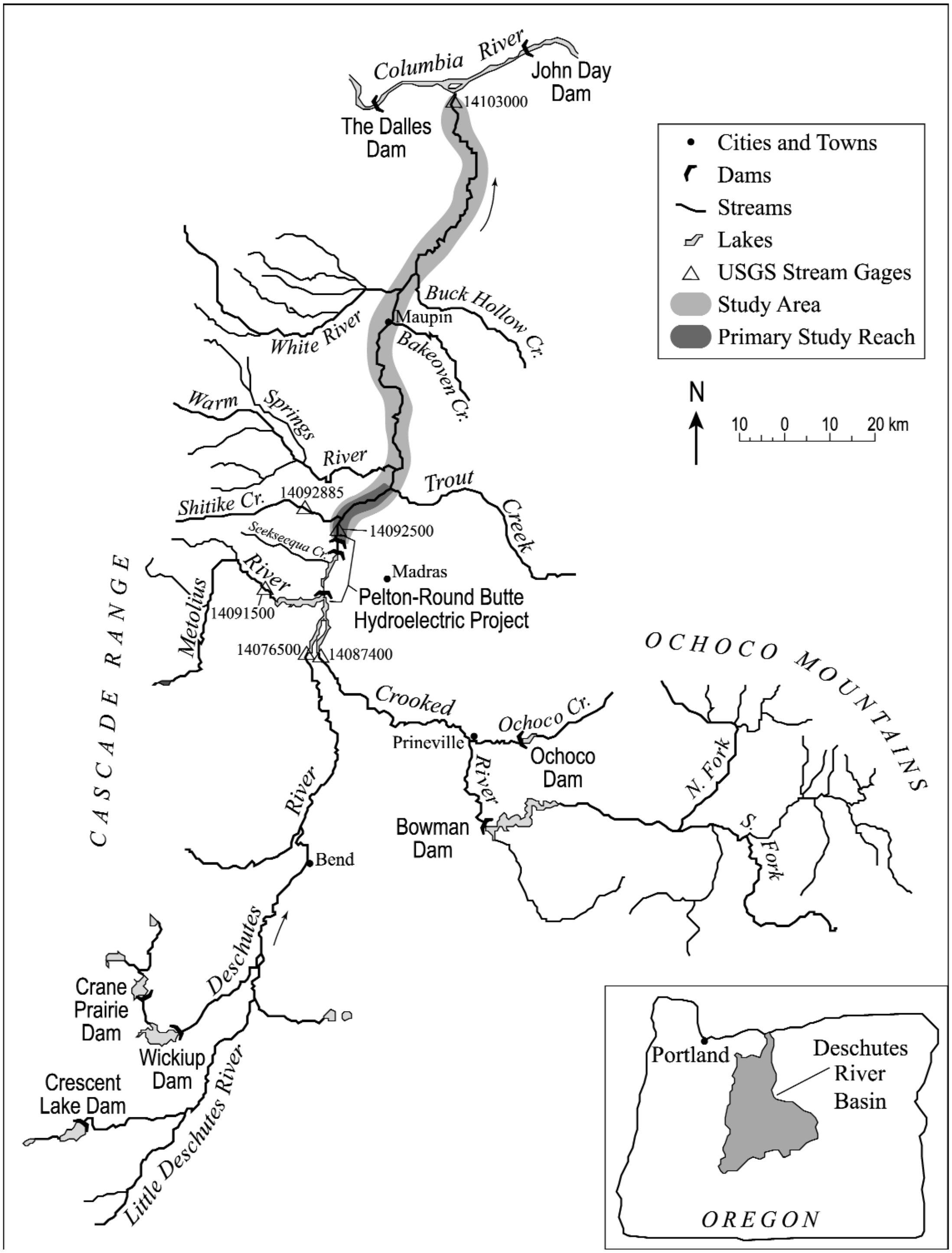

Figure 1. The Deschutes River basin. Base map from *Aney et al.* [1967].

larger study area, a primary study reach, extending 21 km between the Reregulating Dam and Trout Creek tributary (RM 87.3), was chosen based on the premise that the effects of the Project would be most pronounced in the reach closest to the dams. All field data used in the bedload transport study were collected within this primary study reach; the channel-bed texture study included both the primary study reach and the entire study area.

Geomorphic and Hydrologic Setting

The lower Deschutes River is deeply incised into a 600-800 m deep bedrock canyon comprised of volcanic, volcaniclastic, and sedimentary units [*O'Connor, Grant and Haluska*, this volume]. Upstream, the upper Deschutes River basin drains highly porous and permeable Pliocene and Pleistocene basalt fields, which are fed by snowfields through a relatively undissected and poorly integrated stream network with many springs [*Manga*, 1996; *Gannett et al.*, this volume]. River widths in the lower river range from 10–170 m, with narrower sections reflecting reaches where the river flows through more resistant rock formations. Floodplains and terraces are rare in these confined reaches but more numerous in unconfined sections. Islands and submerged bars are key morphologic and ecologic features and are commonly associated with tributary fans and channel-margin expansions and constrictions [*Curran and O'Connor*, this volume]. Exposed bars are rare. For the purposes of this study, islands were defined as vegetated mid-channel or channel-margin deposits bounded by water. Vegetation on islands included any combination of trees, shrubs, and grasses. Trees on islands were not cored; however, ages ranged from saplings to decades old. Bars were defined as unvegetated mid-channel and channel-margin deposits usually submerged at mean annual flow.

The quantity, composition, and source of sediment delivered to the lower Deschutes River has varied significantly over geologic and historic time scales [*O'Connor, Grant and Haluska*, this volume]. Recent, proximal sediment sources include canyon-wall landslides and rock falls, and fluvial erosion of previously deposited material from both the main channel and its tributaries. The main-channel bed-material is basalt and andesite ranging in size from silt to boulders, with the majority of particles being gravel and cobbles. For most of its length, the lower river has very low sinuosity (<1.2, J. E. O'Connor, U.S. Geological Survey, written communication, 2002) and a very uniform channel gradient [approximately 0.23%, *Aney et al.*, 1967; *McClure*, 1998].

Native riparian species include white alder (*Alnus rhombiofolia*), willow (*Salix spp.*), sedges, rushes, and perennial grasses [*Nehlsen*, 1995]. Although several macrophytes populate portions of the lower Deschutes, coontail (*Ceratophyllum demersum*, identification, S. Gregory, Oregon State University, oral communication, 1998), also known as hornwort, is by far the most abundant, and is concentrated in the reach closest to the Project. This floating macrophyte occupies zones of shallow, slow-moving water [*Haslam*, 1987] and is anchored by shoots penetrating bed material.

The lower Deschutes River experiences only small seasonal variations in discharge because of large groundwater contributions [*Gannett et al.*, 1996; *Gannett et al.*, this volume]. There are two active U.S. Geological Survey (USGS) stream gaging stations on the mainstem lower Deschutes River: station 14092500 (Deschutes River near Madras, Oregon) located at RM 100.1 just downstream from the Reregulating Dam, and station 14103000 (Deschutes River at Moody near Biggs, Oregon) located at RM 1.4 near the mouth (Figure 1). Flow duration curves from the Madras station, for water years 1925-1955 and 1966-1996, illustrate the extraordinary uniformity of river flows (Figure 2). The mean daily discharge with a 90% exceedance probability is less than two times the 10% exceedance probability. The difference between the 1% and 99% exceedance probability discharges is less than a factor of three.

Since the Madras gage began operation in 1924, the lower Deschutes River has experienced two exceptionally large floods in December 1964 and February 1996 (Table 1). Both floods occurred as the result of rain-on-snow events. Round Butte Dam caught the peak of the December 1964 flood, which filled the reservoir for the first time, almost a year ahead of schedule.

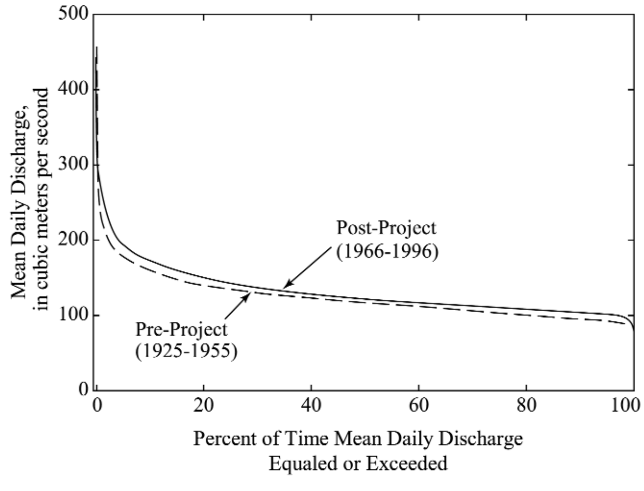

Figure 2. 30-year flow duration curves for pre-Project (water years 1925-1955) and post-Project (water years 1966-1996) time periods.

Table 1. Stream gage and streamflow characteristics of the lower Deschutes River.

	Madras gage (14092500)	Moody gage (14103000)	Reference
Stream gage characteristics			
Period of Record	Jan 1924-June 1933 Aug 1929-Nov 1956 Nov 1957-present	Oct 1897-Dec 1899 Jul 1906-present	1, 2
Location (River Mile)	102.8 102.4 100.1	1.4	1, 2
Drainage Area (km^2)	20,274	27,195	1
Streamflow characteristics (m^3/s)			
Mean Annual Flows			
Range	101-174	121-209	4, 5
Average	128	163	4, 5
Maximum Recorded Flows [a]	637	1,991	1
Largest Flood Peaks [b]			
February 8, 1996			
Instantaneous flow	541	1,991	1
Mean daily flow	504[c]	1,821	1
December 1964	December 28, 1964	December 22, 1964	3
Instantaneous flow	447	1,906	1, 3
Mean daily flow	428	1,767 [d]	3
Minimum Recorded Flows [a]	26	68	1

[a] Instantaneous flow regardless of whether due to storm event or anthropogenic causes.
[b] Flow resulting from storm events only.
[c] Original provisional data listed this value as 510 m^3/s, which was used in our calculations in 1996. Later final data listed this value as 504 m^3/s. The change had a negligible effect on our calculations.
[d] Occurred on December 23, 1964 [*US Department of the Interior*, 1965].

References: 1. *Hubbard et al*. [1997]; 2. *U.S. Department of the Interior* [1994]; 3. *U.S. Department of the Interior* [1965]; 4. U.S. Department of the Interior, U.S. Geological Survey, http://oregon.usgs.gov/www_mans95_dir/man 14092500.html, October, 1997; 5. U.S. Department of the Interior, U.S. Geological Survey, http://oregon.usgs.gov/www_mans95_dir/man 14103000.html, October, 1997.

River Regulation

The Deschutes River is regulated by eight major water storage projects (Figure 1, Table 2) and numerous irrigation diversions; the dams in the basin retain a total of $128 \cdot 10^7$ m^3 of water, 76% of which is permitted annual active storage (though on average only 38% is used). *Permitted annual active storage* is the volume of water that a dam is allowed to retain, and then release at a different time. *Average annual active storage*, or the average storage used, is the actual annual average difference between the minimum and maximum pool elevation recorded each year for a dam's reservoir (D. Ratliff, Portland General Electric, written communication, 2002). The Project's Round Butte Dam impounds the basin's largest reservoir, Lake Billy Chinook, holding over 40% of the total water stored in the basin. However, this dam is responsible for only 11% of the basin's average annual active storage. The Pelton and the Reregulating Dams have no annual active storage. The purpose of the Reregulating Dam is to provide constant discharge to the lower Deschutes River while allowing daily peaking power production from Pelton Dam upstream. To accomplish this, the Reregulating Dam stores water and evens flow on a daily basis. Downstream of the Project, the Deschutes River flows uninterrupted to its confluence with the Columbia River.

Table 2. Storage characteristics of major water storage projects in the Deschutes River basin.

Project (Reservoir)	River	Year Construction Began	Purpose of Dam	Total Storage (10^7 m^3)	Permitted Annual Active Storage (10^7 m^3)	Average Used Annual Active Storage (10^7 m^3)	Drainage Area (km^2)
Ochoco (Ochoco)	Ochoco Creek	1918 [a, b]	Flood control Irrigation	5.92 [a ,b]	5.7 [a, b]	3.26 [c]	750 [b]
Crane Prairie (Crane Prairie)	Deschutes	1922 [d]	Irrigation	6.82 [d, e]	6.6 [d]	3.45 [c]	660 [d, e]
Crescent Lake (Crescent Lake)	Crescent Creek	1922 [d, f]	Irrigation	11.3 [e, g]	11 [e]	3.62 [c]	150 [e]
Wickiup (Wickiup)	Deschutes	1939 [h]	Irrigation	24.7 [g, h]	24.7 [h]	18.0 [c]	660 [g, h] 1,040
Pelton (Lake Simtustus)	Deschutes	1956 [i]	Hydroelectric	3.82 [i]	0.46 [i]	0 [i]	19,950? [e]
Pelton Reregulation	Deschutes	1956 [i]	Flow reregulation Hydroelectric	0.43 [i]	0.31 [i]	0 [i]	20,250 [j]
Bowman (Prineville)	Crooked	1958 [b, k]	Flood control Irrigation	19.1 [b, k]	19 [b, k]	9.38 [c]	7,280 [b]
Round Butte (Lake Billy Chinook)	Deschutes	1962 [i]	Hydroelectric	56.1 [i]	30 [i]	5.42 [l]	19,410 [j]
TOTAL				128	97.8	48.5	

[a] U.S. Army Corps of Engineers, unpublished data (1959).
[b] *U.S. Department of the Interior, Bureau of Reclamation* [1966].
[c] Wayne Skladal, Central Region WRD, Bend, Oregon, written communication, 1999.
[d] K. Gorman, Watermaster, Central Oregon Irrigation District, Bend, Oregon, oral communication, 1997. Original dam had around the same storage capacity as listed. The dam was rebuilt from 1943 - 1947 improving its structural support. This may refer to the same rebuild that other references cite as occurring in 1940. The hydrologic drainage boundary is uncertain due to inter-basin groundwater exchange.
[e] *Johnson* [1985].
[f] G. Cartwright, Field Supervisor, Tumalo Irrigation District, Bend, Oregon, oral communication, 1997. Storage values are for post-1956.
[g] Northwest Power Planning Council, unpublished data (1986). Values given under total storage are maximum capacity.
[h] *U.S. Department of the Interior, Water and Power Resources Service* [1981].
[i] Portland General Electric, unpublished data (1996).
[j] *Hubbard et al.* [1997].
[k] U.S. Army Corps of Engineers, unpublished data (1961).
[l] Portland General Electric, PGE Hydro Operations Records for Round Butte Dam: 1966-2001, Portland General Electric Company, Portland, Oregon.

Upstream of the Project near Bend, substantial quantities of water are diverted for irrigation, with as much as 94% of monthly streamflow being diverted at the height of the irrigation season [*Fassnacht*, 1998]. However, about 85 m^3/s, or $270 \cdot 10^7$ m^3, of groundwater is estimated to enter the Deschutes system annually below major irrigation diversions and above Lake Billy Chinook [*Gannett et al.*, 1996; *Gannett et al.*, this volume]. This is over five and a half times the annual active storage used in the basin. As a result, even with the presence of the water storage projects and irrigation water withdrawal systems upstream, the lower Deschutes River has been able to maintain its historically stable discharge.

METHODS

Diverse methods were used to examine the Project's effect on the lower Deschutes River. We focused our data collection and analysis on those physical processes and aspects of channel adjustment that we predicted to be most sensitive to Project influences over the time since the Project's construction. Because of the different methods, study locations, and timescales of analysis used, we discuss methods and data analysis separately for each of the study components: bedload transport, channel morphology, and channel-bed texture. The results, which follow the methods section, are organized in a similar fashion.

Bedload Transport

Within the primary study reach, five sites were selected (sites B, D, E, H, and I; Figure 3), representing three hydraulic environments characteristic of the lower Deschutes River: straight, contraction, and expansion zones (Figure 4). Straight zones are reaches where the channel banks are roughly parallel (Figure 4a); contraction zones are those where the channel width decreases abruptly downstream (Figure 4b); and expansion zones are reaches where the channel widens abruptly downstream (Figure 4c). In the Deschutes River channel, contractions and expansions are often the result of tributary alluvial fans constricting the main river channel [*Curran and O'Connor*, this volume; e.g., Figure 4b].

In 1995, cross sections were measured at each site along four to seven transects oriented perpendicular to the main direction of flow (Figure 5); the number of transects measured per site depended on the site's morphologic complexity. Where the water was more than 0.5 m deep, cross-sectional profiles were measured using an Acoustic Doppler Current Profiler (ADCP) mounted on a jet boat. Horizontal positions were calculated from bottom tracking measurements taken along sighted cross sections. Depth resolution of the ADCP is approximately 0.1 m for a single beam [*RD Instruments,* 1996]. The instrument has four beams, each oriented at 20° from vertical. Estimated water depths at the time of measurement were around 2 m, resulting in a relatively small footprint delineated by the four beams. We made four passes per cross section with the jet boat to obtain more data points and to improve our ability to estimate water depth and therefore cross-section shape. On dry land or where the water was less than 0.5 m deep, elevations were surveyed using an electronic total-station. Vertical accuracy of cross-section points gathered by the electronic total-station is judged to be better than 0.1 m.

Surface particle-size distributions were measured for each site using a modified pebble-count technique [*Wolman*, 1954]. Approximately 100 particles per site were measured along a survey tape oriented parallel to streamflow. Sampling took place on shallow submerged bars, and along

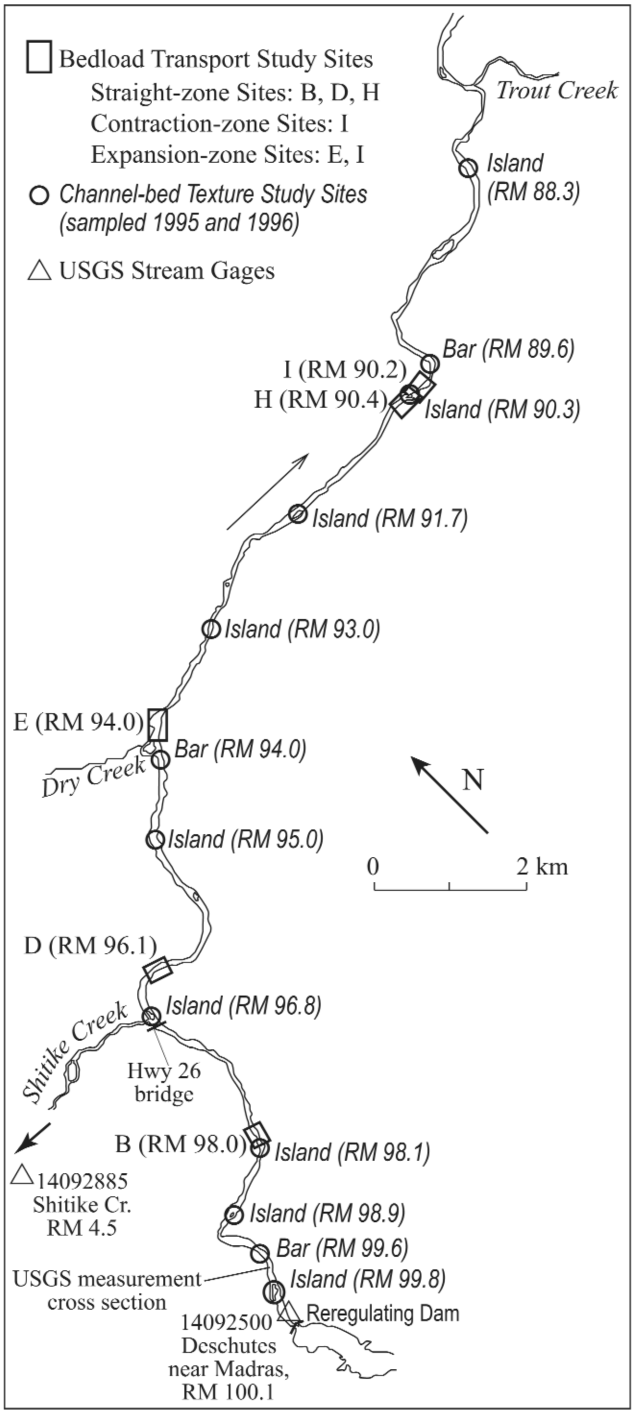

Figure 3. Primary study reach and bedload transport and channel-bed texture study sites. Base map from *Appel* [1986].

island and channel margins within or adjacent to each site; deep, fast moving water precluded sampling the channel bed near the thalweg. Visual underwater inspection of deeper

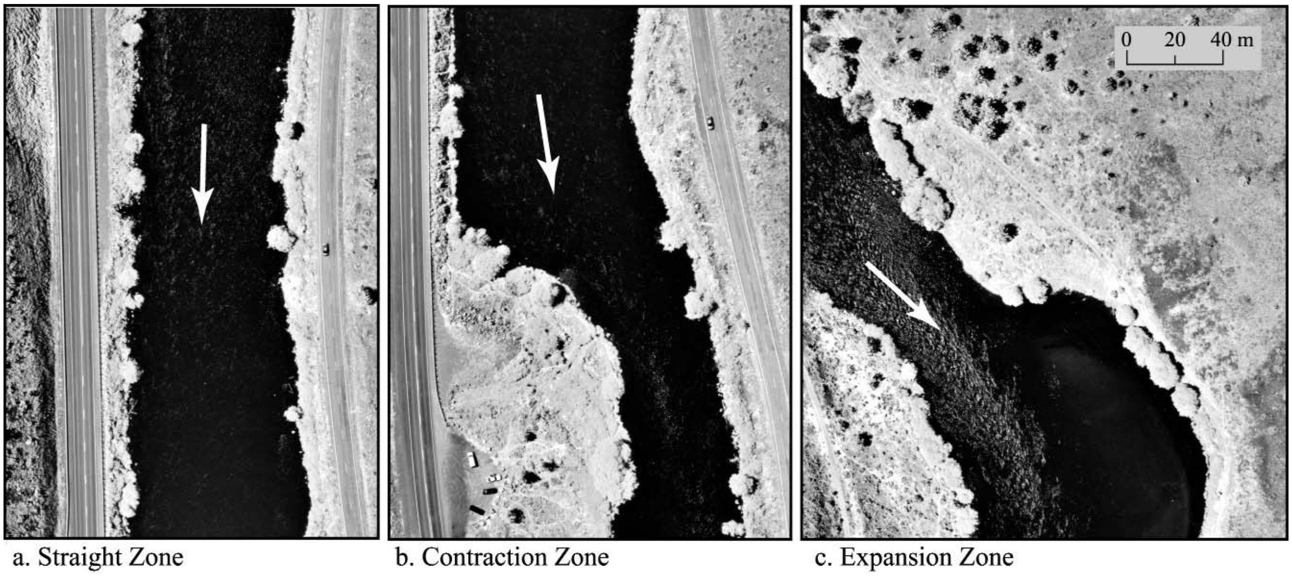

Figure 4. Three hydraulic environments found on the lower Deschutes River: (a) straight, (b) contraction, and (c) expansion zones.

regions of the river suggested that the range of grain sizes on the channel bed at each site was relatively narrow, and reasonably well represented by marginal deposits. These observations are supported by the results of a channel-bed texture study [*McClure*, 1998].

Low-flow water surface elevations were measured during the summer 1995 cross-section surveys. Following the record flood in February 1996, we revisited all sites and surveyed the flood's high-water line against the 1995 elevations using a stadia rod and hand level. Discharges for September 1995 and February 1996 (the dates for which we obtained field measurements of water surface elevation) were derived from mean daily flow data from the Madras gage (station 14092500) for the site located above Shitike Creek confluence (Site B, Figure 3) and from the sum of the discharges measured at the Madras and Shitike Creek gages (Shitike Creek values from station 14092885, Figure 1) for sites located downstream of the Shitike Creek confluence (Sites D, E, H, and I; Figure 3). Discharges for September 1995 ranged from 96 to 105 m^3/s over the five sites; for February 1996, the range was from 510 to 586 m^3/s based on provisional data from the USGS.

Entrainment and Transport of Bedload. Mean shear stresses (τ) were estimated for each site by combining field measurements with the one-dimensional step-backwater curve model HEC-RAS [*U.S. Army Corps of Engineers*, 1995 a,b]. Shear stresses were calculated by using hydraulic mean depth values generated by HEC-RAS, and the relation

$$\tau = \gamma_f \bar{d} S_e \tag{1}$$

where τ is shear stress, γ_f is the specific weight of the fluid (water), $\bar{d}$ is hydraulic mean depth ($\bar{d} = A/T$ where A is area and T is top width), and S_e is the downstream slope of the energy grade line, or energy slope. Energy slope was determined by fitting a regression line through "energy gradeline points", the sum of the average velocity head at a transect

$$h_{v_{avg}} = V_{avg}^2/2g \tag{2}$$

(where V_{avg} is the average velocity and g is gravitational acceleration), and a regression line fit through water surface elevations measured in the field. Hydraulic mean depth was used instead of hydraulic radius to be consistent with parameters used in the bedload transport model. The shear stress required to entrain the median particle diameter of the channel-bed surface material, or critical shear stress (τ_{cr50s}), was determined for each study site from *Shields* [1936],

$$\tau^*_{cr50s} = \frac{\tau_{cr50s}}{(\rho_s - \rho_f) g D_{50s}} \tag{3}$$

where τ^*_{cr50s} is dimensionless critical shear stress, or Shields stress, for the median particle diameter of the channel-bed

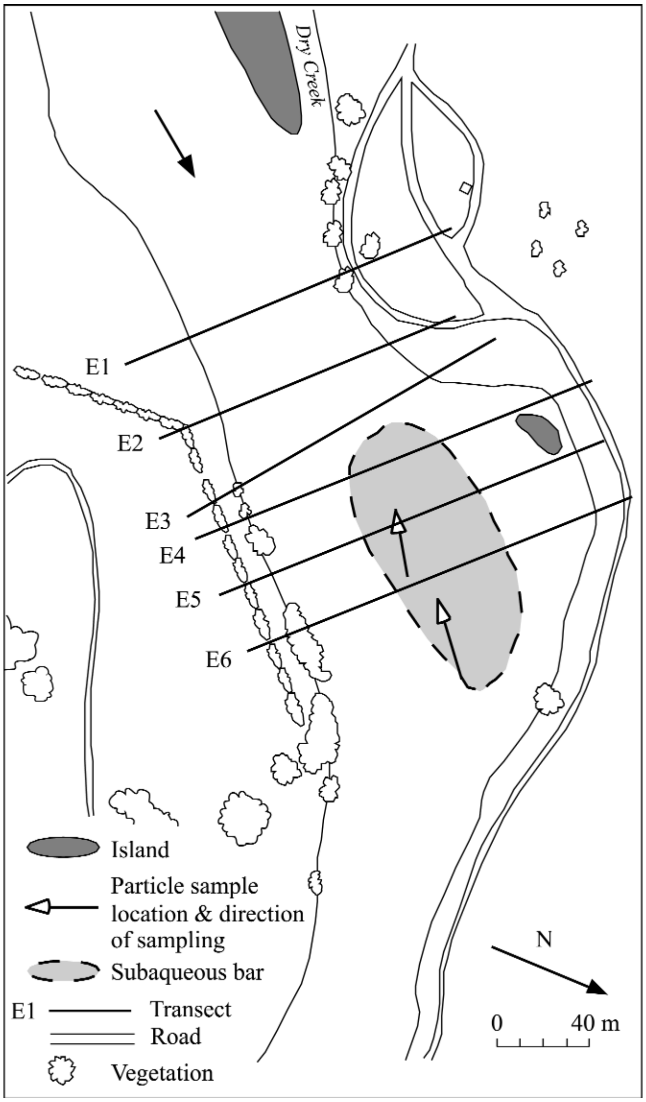

Figure 5. Example transect layout (Site E).

surface (D_{50s}), ρ_s is the density of the sediment, ρ_f is the density of the fluid (water), and g is gravitational acceleration. For particles coarser than sand, Shields stress is essentially constant; we used a value of $\tau^*_{cr50s} = 0.047$, consistent with that used by *Meyer-Peter and Mueller* [1948] for coarse-bedded rivers. After HEC-RAS was calibrated to September 1995 and February 1996 discharges and their associated measured water surface elevations, the model was run for a range of discharges, 100-500 m^3/s, intermediate to the discharges used for calibration. Shear stress was plotted against discharge to construct a rating curve for each site (e.g., Figure 6). Critical shear stress was then calculated (Equation 3) for each site and superimposed on the site's rating curve to estimate the discharge required to produce threshold transport conditions (critical discharge, Q_{cr}) at that site (Figure 6).

We analyzed the sensitivity of the calculated critical discharges and corresponding shear stresses to important parameters—the energy slope (S_e), median particle diameter of the channel-bed surface (D_{50s}), and Shields stress for the median diameter of the channel-bed surface (τ^*_{cr50s}). The parameters were changed one at a time by ± 10% while all other independent parameters were held constant. The energy slope was varied by plus or minus one half of a standard deviation to maintain similitude with observed values. Standard deviation was calculated by using slopes derived from water surface elevations measured at all bedload transport study sites. The effect of the parameter variations on critical discharge was then evaluated. To test the robustness of the model to changes in more than one parameter at a time, the three parameters evaluated were varied simultaneously to either increase or decrease critical discharge.

Rating curves of predicted bedload transport rate (Q_S) versus water discharge (Q) were constructed for each site for a range of discharges. Values for Q_S were calculated by combining field measurements with hydraulic data derived from the HEC-RAS model, and inputting them, , to Parker's one-dimensional bedload transport model for gravel mixtures, as described in *Fassnacht* [1998] and *Parker* [1990]. Bedload transport rates were calculated based on the assumptions that sediment supply was unlimited and channel-bed grain size remained constant through time.

Frequency and Magnitude of Streamflow and Bedload Transport. Annual and 30-year flow duration curves were constructed from mean daily flow data for the period 1925-1996 to evaluate changes in flow frequency with time. The 30-year curves specifically compare the pre-Project (1925-1955) and post-Project (1966-1996) time periods.

Results from the hydraulic, sensitivity, and bedload transport analyses were further evaluated using historical streamflow data to make a first-order approximation of the frequency and magnitude of bedload transport in the primary study reach. The largest calculated critical discharge value for all sites examined was used in this analysis because, at this discharge, bedload transport should occur at all sites. The sensitivity analysis, where the three tested parameters were varied simultaneously, provided a range of what we considered the maximum deviation of the critical discharge value. These "alternate" lowest and highest critical discharge values were also evaluated in determining the frequency of bedload transport, to determine how sensitive results were to uncertainties in the flow analysis. The frequency of bedload

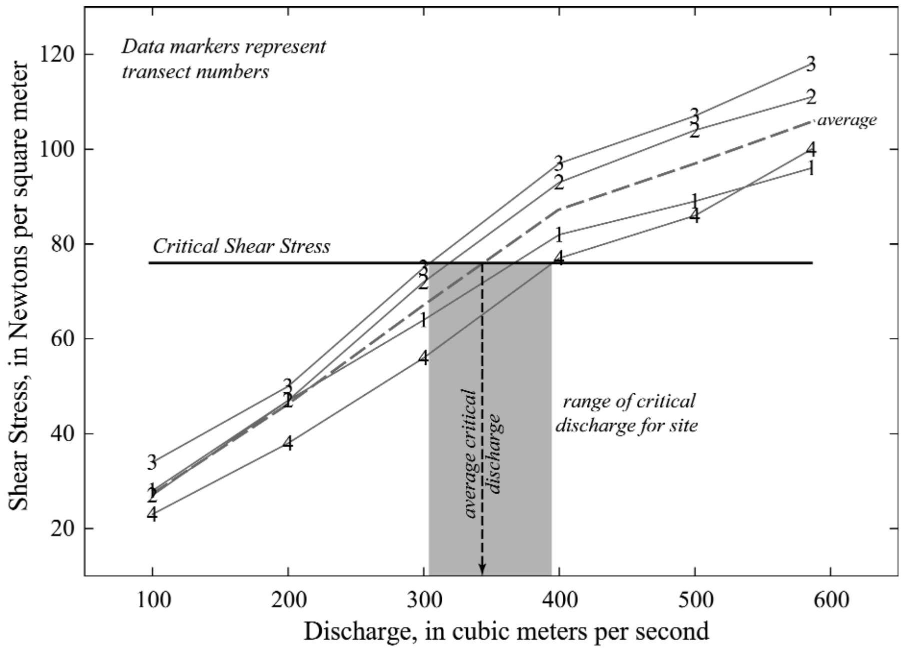

Figure 6. Example discharge (Q) vs. shear stress (τ) rating curve (Site B).

transport was calculated using historical daily streamflow records by determining the number of days over the period of record during which the calculated critical discharge (or the alternate values) were equaled or exceeded.

The quantity of bedload predicted to have moved per day and per water year for water years 1925 to 1996 was calculated at Site B using the sediment rating curve. Days during which bedload transport was predicted to have occurred were called "transport days," and a continuous series of these days was called a "transport event." Bedload transport rates during the data-gathering phase of this study were assumed to be relatively consistent (and low) with the exception of the transport that occurred during the February 1996 flood.

Project Effects on Streamflow and Bedload Transport. Determination of Project effects on streamflow is confounded by the presence of five dams (Table 2) and six major flow diversions upstream of the Project. In addition, water storage (both natural and anthropogenic), water diversions, irrigation return-flow, climate change, and interbasin groundwater exchanges influence the pattern of streamflow in the basin. Because of these confounding factors, we compared streamflow entering and exiting the Project to evaluate the Project's effects. Inflow-outflow comparisons are valuable because they provide one of the best estimates of the effect of a dam on downstream discharge and, consequently, on bedload transport.

Historical streamflow and reservoir storage data and the results of our previous analyses were used to examine the effects of the Project on water and sediment discharges. Hydrographs of mean daily inflow and outflow were developed for the Project for post-dam storm events whose discharge exceeded calculated threshold transport conditions.

Inflows to the Project were calculated using two methods. The first employed reservoir elevation data and elevation-storage rating curves [Duke Engineering and Services Consulting, Portland, Oregon, written communication, 1996; *Fassnacht*, 1998]. For storm events where these data were not available, a second method was used; inflows were estimated by adding together discharges from the three main rivers tributary to Lake Billy Chinook: the Crooked, the upper Deschutes, and the Metolius Rivers (see Table 3 for details of gage locations). A correction factor was then applied to this sum to compensate for otherwise unaccounted-for discharges entering between the gages and Round Butte Dam. These discharges derive from an area equal to 4% of Lake Billy Chinook's total drainage area. To determine the correction factor, we selected storm events where reservoir elevation data were available and we calculated inflow using both the elevation-storage rating curve and the sum of the discharges from the three upstream USGS gages. The average of the differences in results was used as the correction factor.

Table 3. Deschutes River gaging stations used to determine streamflow into Lake Billy Chinook.

River	Location	USGS Station	Reference
Crooked	below Opal Springs, near Culver, Oregon	14087400	*1*
upper Deschutes	near Culver, Oregon	14076500	*2*
Metolius	near Grandview, Oregon	14091500	*3*

References:
1. U.S. Dept. of the Interior, U.S. Geological Survey, http://water.usgs.gov/swr/OR/data.modules/hist.cgi?statnum =14087400, October, 1997;
2. U.S. Dept. of the Interior, U.S. Geological Survey, http://water.usgs.gov/swr/OR/data.modules/hist.cgi?statnum =14076500, October, 1997;
3. U.S. Department of the Interior, U.S. Geological Survey, http://water.usgs.gov/swr/OR/data.modules/hist.cgi?statnum =14091500, October, 1997.

From the Project inflow and outflow hydrographs, the predicted quantity of bedload transported through the sites was calculated using sediment rating curves derived from the bedload transport analysis. Bedload transport calculations for sites located below Shitike Creek confluence and for all transport events except those in 1996, reflect only the bed material moved by streamflow as measured at the Madras gage, since Shitike Creek, which joins the Deschutes upstream of Site D, was ungaged during most transport events.

Channel Morphology

Cross-section measurements have been collected by the USGS at the 'Deschutes River near Madras' gage station (14092500) from January 1924 to the present. These measurements were analyzed for changes in channel-bed elevation and cross-sectional area from 1924-1998. Movement of the gage and associated cableway twice in connection with dam construction complicates comparison of channel change between pre- and post-dam time periods. Movement of the measurement cross-section occurred before any dams in the Project were closed, however. Locations and time periods over which measurements were made for the three locations of the Madras gage are shown in Table 1. Channel changes described in this analysis are not meant to represent channel change experienced over the entire study area. Measurement cross-sections are specifically chosen for their stability and are, therefore, expected to show less change than elsewhere in the river. The present location of the gage, however, is representative of the river in the primary study reach.

Minimum streambed elevations from 1924-1998 were determined to evaluate the record for evidence of long-term degradation or aggradation at the gage site [*Smelser and Schmidt*, 1998]. In addition, cross-sectional areas were calculated for every third USGS cross-section measurement from 1957 to 1998. Cross sections prior to 1957 were not included because of the pronounced stability (bedrock) of the streambed at the two gage locations during this time period. Areas were calculated for the part of the cross-section existing below 2 m from an arbitrary datum. This allowed for consistent comparison of data across the range of measured discharges. At some of the larger discharges, cross-section measurement data for one stream bank or the other did not begin until 1-1.5 m or more below the datum. Simple linear regressions tested whether observed changes were significant. Temporal trends were examined by looking at changes in cross-section shape and area for measurements bracketing individual high discharge events. Cross-section measurements were also evaluated every 57 m^3/s (2000 ft^3/s) increment in flow, starting at 113 m^3/s, to investigate thresholds of general bed mobility over the cross section.

Channel-Bed Texture

Because islands and bars represent the dominant depositional features in the river, they were sampled to analyze longitudinal trends in bed material size. Sampled sites included islands and bars in comparable hydraulic settings [*Kondolf*, 1997] along which sampling grids could be safely established under low flow conditions. Around each island, four distinctive geomorphic environments were sampled: the head (upstream end), side (abutting main flow), side channel (side bordering secondary channel), and tail (downstream end) (Figure 7). Head and tail environments of selected bars were also sampled (Figure 7). For hydraulic consistency, results presented here focus on comparison of grain-size distributions from heads of islands and bars. Analysis of other geomorphic environments shows similar trends [*McClure*, 1998].

Nine islands and three bars were sampled in the primary study reach in the summer of 1995 (Figure 3) and then resampled in the summer of 1996 to document changes following the February 1996 flood. Eleven island heads in the lowermost 140 km of the river were also sampled during the summer of 1996 to extend the analysis downstream to the Columbia River (Figure 8).

Surface bed-material was sampled at each site by measuring the intermediate (b-axis) particle diameter for three standard 100-particle pebble counts conducted on three overlap-

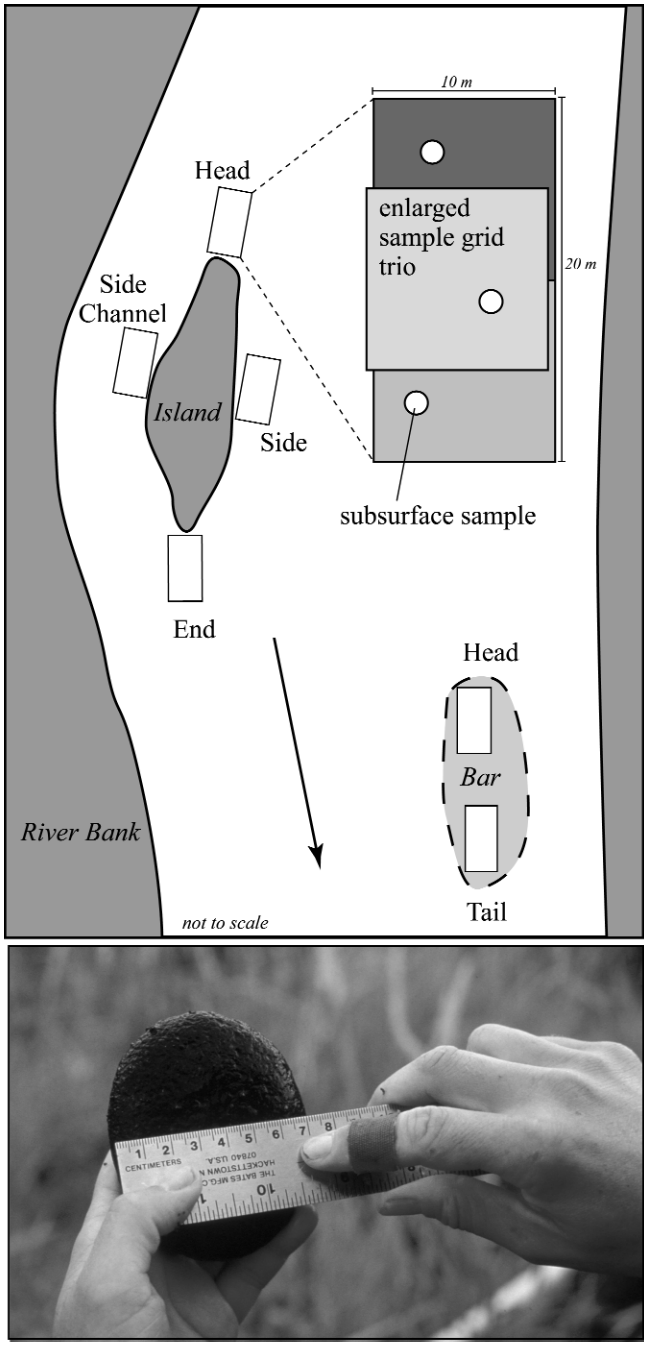

Figure 7. Schematic of sampling design at vegetated island and submerged bar. Photo of b-axis measurement of surface particles by Heidi Fassnacht.

ping 10 m by 10 m grids (Figure 7) [*Wolman*, 1954]. Smaller particles were binned into a < 2 mm category in the field. Sample grids were centered along a line through the island or bar, parallel to flow, and spaced no more than 3 m from vegetated island perimeters (Figure 7). The use of a grid system insured independence of samples. Overlapping of surface sampling grids allowed for the testing of spatial autocorrelation at lag distances less than 1 m. Sampling environments showed neither clear nor consistent gradients to suggest bias introduced by sampling more particles from the central area of a 10 m by 20 m grid. Along with each particle measurement, the presence or absence of the macrophyte *C. demersum* was noted (Figure 9). Since the plant can trap fine sediment on the bed surface, it was necessary to account for its abundance in later analyses.

Although *Wolman* [1954] suggested that measuring 100 particles was sufficient for sampling, *Rice and Church* [1996] recommended 400-stone samples to improve estimates of all percentiles to within a tenth of a phi unit [$\Phi = -\log_2$(particle diameter in mm)] for 95% confidence limits. In this component of the study, pebble counts from a single area were pooled to form individual pebble counts of 200 to 600 particles for each site. This effectively reduced the sample number to one for each island or bar head and, therefore, restricted the total number of sampled island and bar heads in both years to twenty-three. As a result, statistical methods were focused on estimating longitudinal variability between island and bar heads, rather than variability between pebble counts at each island or bar head.

Grain-size measurements from tributaries were used to identify local sources of sediment that could affect textural patterns within the mainstem. Tributaries sampled include Shitike Creek in the primary study reach and thirteen tributaries farther downstream (Figure 8). Pebble counts of 400 particles were conducted along reaches of two to ten channel widths by pacing back and forth between the bankfull channel margins. For each tributary, sampling was conducted near the confluence with the lower Deschutes but above the zone influenced by backwater from the mainstem.

The subsurface of the bed was also sampled at each site on the mainstem where surface sampling was conducted. The armor layer, extending to the depth of the largest surface particle, was removed by hand, and subsurface material extending to a depth between one to two times the thickness of the armor layer was scooped into a bucket. To prevent washing of fine sediment downstream, a sawed-off 55-gallon barrel cylinder was worked vertically into the submerged bed. Water, collected in the scoop, was also added to the bucket to retain finer particles suspended during the sampling process.

At least one subsurface sample was collected beneath each pebble count grid in the summer of 1995 (Figure 7). To expedite sampling in the summer of 1996, only a sample from the middle grid was obtained. For both 1995 and 1996,

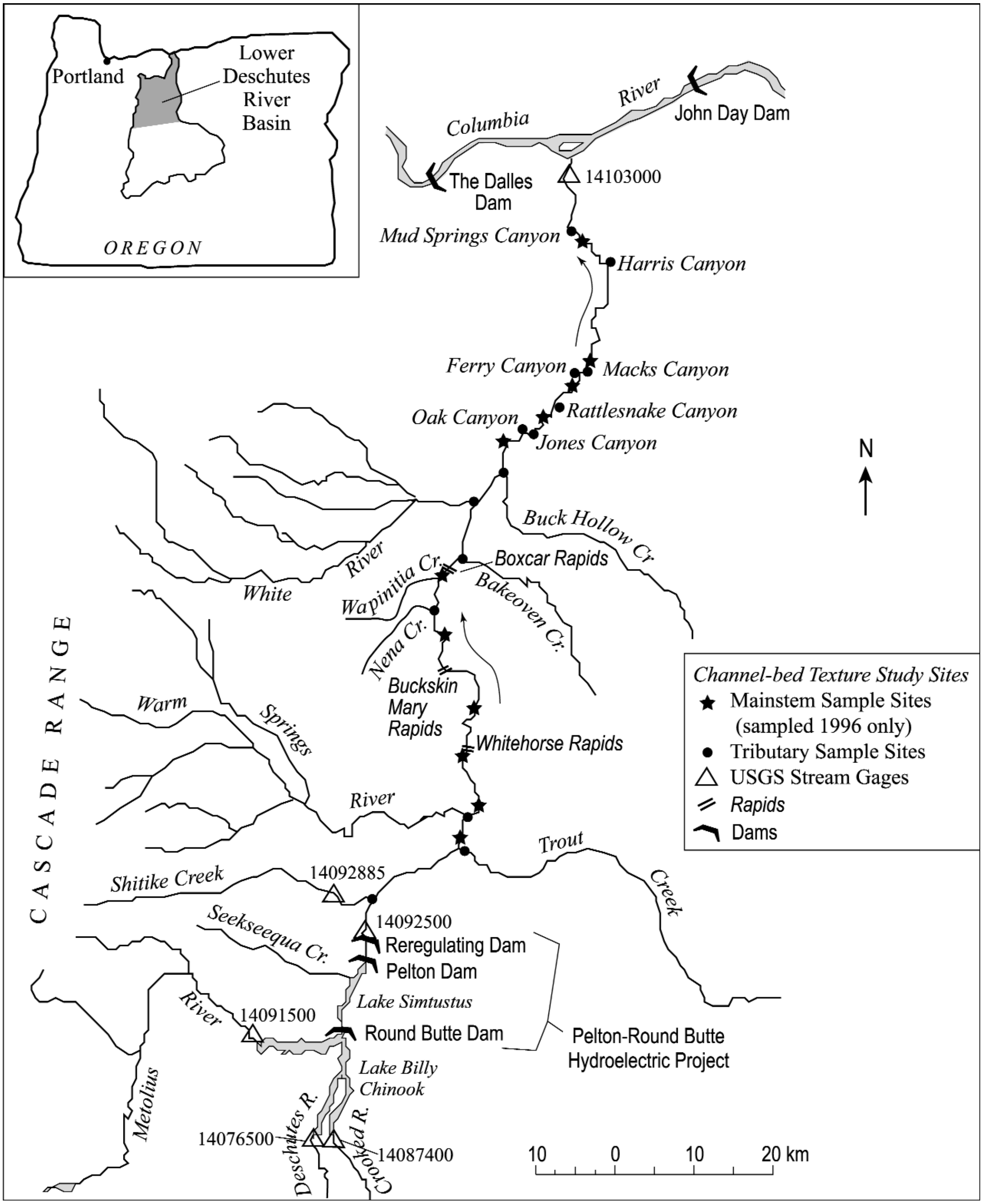

Figure 8. Lower Deschutes River showing bed material sampling locations for mainstem and tributaries. Base map from *Aney et al.* [1967].

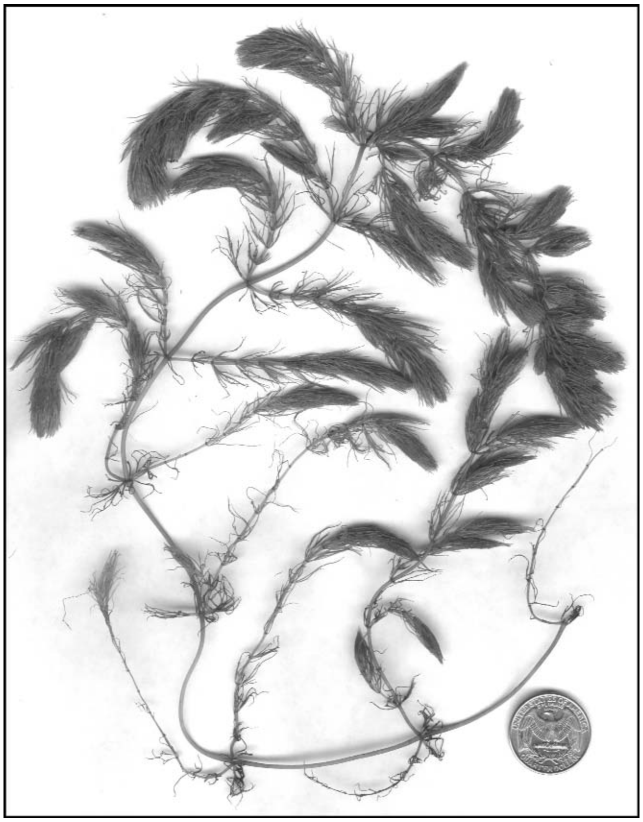

Figure 9. The macrophyte *Ceratophyllum demersum*. Common names are coontail and hornwort. Photo by Mike Naylor, Maryland Department of Natural Resources.

individual samples averaged about 20.3 kg by dry weight. Bulk samples from 1995 were pooled to form samples averaging 60.9 kg for each site. All samples were dried in the laboratory and sieved using a progression of U.S. Standard sieves spanning the range from 101.6 mm to <0.063 mm.

For surface and subsurface samples, percentiles of the grain-size distribution (D_5, D_{16}, D_{25}, D_{50}, D_{75}, D_{84}, D_{95}) on the phi scale were computed by site and then converted to millimeters. From these values, the armoring ratio was calculated for each site as

$$D_{50\ surface}\,(\mathrm{mm})/D_{50\ subsurface}\,(\mathrm{mm}) \quad (4)$$

Trask sorting coefficients were computed as

$$[D_{75}\,(mm)\,/\,D_{25}\,(mm)]^{1/2} \quad (5)$$

with higher values indicating poorer sorting [*Krumbein and Pettijohn*, 1938].

We developed statistical models to evaluate longitudinal trends in grain size and changes following the 1996 flood, while accounting for the abundance of *C. demersum* at each site. Because grain-size percentiles in a single grain-size distribution are correlated, only D_{50} values were tested statistically. The surface, subsurface, and armoring data were analyzed separately using multiple linear regression. Separate statistical analyses were conducted for data from the primary study reach (1995 and 1996) and for that from the entire study area (1996 only).

Analysis of the surface grain-size, subsurface grain-size, and armoring data for the primary study reach and entire study area resulted in six statistical models. Each model of the three data sets included variables for location (River Kilometer, distance upstream from the mouth in kilometers) and year. Since these two variables were designed to identify spatial and temporal patterns rather than to build a predictive model, they were not dropped from the model even if they were not statistically significant. Models for surface grain size also included a variable for the abundance of *C. demersum*; however, this variable was dropped from the model if it was not significant. Interactions between variables were tested at the 0.05 significance level. For each model, interaction terms with 2-sided p-values exceeding 0.05 were dropped. Following these guidelines, final models were developed. For each final model, the effect of influential points was evaluated. Significance of variables in the final models was assessed at the 0.05 significance level.

RESULTS

Bedload Transport

Entrainment and Transport of Bedload. A narrow range of critical discharges for bed entrainment was calculated for four of the five sites (Sites B, D, E, and I); site-averaged model estimates ranged from 310 to 340 m^3/s as measured at the Madras gage (Table 4). A critical discharge value for Site H could not be determined because the modeled critical shear stress was greater than the largest shear stress in the Q vs. τ curve calculated for the site. Field observations (e.g., fresh gravel deposits) following the February 1996 flood, however, suggest that material was moved through Site H. Consistency of results from the remaining four sites and field evidence strongly suggest that hydraulic values modeled for Site H were over-predicted, and we treated the site as an outlier, removing it from further analysis. For the remaining four sites, the model predicted that bed material would begin to move first in the channel thalweg followed at higher discharges by mobilization of material over the entire cross-section (Table 4) as might be expected.

Table 4. Calculated critical discharge (Q_{cr}) ranges and site-averages as measured at the Madras gage for Sites B, D, E, H, and I. Ranges indicate the extent of variation found in critical discharge values calculated for individual transects at a site. Site-averages are the average of critical discharge values found within the range of values at a site. Bed critical-discharges were calculated as an average critical discharge over the channel bed (i.e. using hydraulic depth). Critical discharges for the channel thalweg are included for comparison (i.e. using maximum depth).

Site	RM	Zone Type [a]	Bed Q_{cr} (m^3/s)		Thalweg[b] Q_{cr} (m^3/s)	
			Range	Site average	Range	Site average
B	98.1	S	310-380	340	250-300	270
D	96.1	S	290-380	320	130-200	160
E	94.0	E	240-490	330	80-420	220
H	90.4	S	[c]	[c]	[c]	[c]
I	90.2	C/E	230-490	310	80-230	120

[a] E = expansion zone, S = straight zone, C = contraction zone
[b] assuming that channel-bed here comprised of same sized material as was measured in shallower water
[c] critical discharge could not be calculated because predicted critical shear stress exceeded the range of shear stresses defined by the Q_{cr} vs τ curve.

We focused on the straight-zone sites (Sites B and D), which most closely fit the assumptions of the one-dimensional hydraulic model. The sensitivity analysis for these two sites showed that individual and simultaneous variation of S_e, D_{50s}, τ^*_{cr50s} did not substantially alter results of the hydraulic analysis. Critical discharges of 270 m^3/s were obtained for both sites when the three tested parameters were simultaneously varied to decrease critical discharge. Values of 420 m^3/s and 500 m^3/s (average 460 m^3/s), were obtained for Sites B and D respectively, when parameters were simultaneously varied to increase critical discharge. These low and high values (270 m^3/s and 460 m^3/s) represent end members of what we will consider the maximum deviation of the critical discharge value for the examined straight-zone sites in the primary study reach.

Bedload transport of all size classes is predicted to occur close to the entrainment threshold modeled for D_{50}-sized bed material. Using Parker's model, we predicted bedload transport of all evaluated particle sizes to begin between ~300 and 400 m^3/s, with transport rates increasing with discharge (Figure 10). Parker's model was derived for conditions when bedload transport is controlled by hydraulic conditions rather than particle availability [*Parker et al.*, 1982]; therefore, bedload transport rates represented here are those that occur following exceedance of threshold transport conditions and disruption of the channel-bed armor layer rather than just during the initial stage of transport.

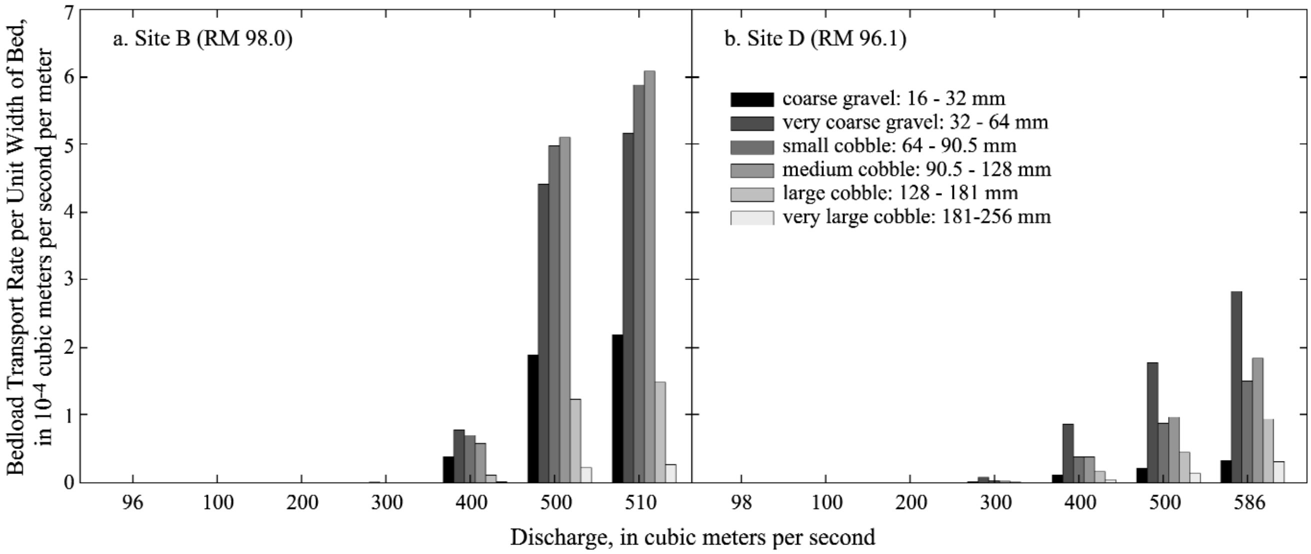

Figure 10. Calculated bedload transport rates per unit gravel-bed width for (a) Site B and (b) Site D.

Frequency and Magnitude of Streamflow and Bedload Transport. Annual flow duration curves showed little change in flow frequency or magnitude over time (Figure 11). Comparison of composite 30-year flow duration curves for the pre- and post-Project time periods similarly revealed that dam effects on hydrology have been slight (Figure 2). These results suggest that Project-induced changes in streamflow did not exist, were subtle, or were operating on time scales other than that of mean daily flow. Differences between the 30-year curves reflect the influence of climate on the two periods: severe drought occurred from the mid-1920s through much of the 1930s, affecting the pre-Project curve, and the largest flood on record affected the post-Project curve. Despite these climatic differences, curves for both time periods are quite similar, underscoring the remarkably stable flow for the Deschutes River prior to and following closure of the Project dams.

Our results predicted that events capable of mobilizing channel-bed material were rare. We found only 26 transport days from 1924 to 1996 (<1% of time) during which mean daily discharge equaled or exceeded 340 m^3/s, the predicted threshold for bedload transport across the sites (Table 5). These estimates are robust with respect to model parameter sensitivity; even our most conservative estimates of parameter values indicated that bedload transport had occurred less than 1% of the time over the 70+-year period of record evaluated (Table 5).

For this same time period, predicted bedload transport rates for Site B generally ranged from 2,000 to 3,000 m^3/yr for the years during which transport was predicted to occur (Figure 12). Two notable exceptions were water years 1965 and 1996 as a result of the December 1964 and February 1996 floods. The 1964 flood was predicted to have transported 6,530 m^3 of bed material and the 1996 flood 14,900 m^3, or 7% and 42% respectively, of all material calculated to have moved through Site B since 1925.

Project Effects on Streamflow and Bedload Transport. Post-Project transport events were predicted to have occurred in December 1964, January 1965, March 1972, February 1982, and February 1996. The 1964 event occurred prior to the Project being fully operational but was included in the analysis because this flood had the largest recorded inflow to the Project (Portland General Electric, 121 S.W. Salmon Street, Portland, OR, unpublished data, 1996), the second highest discharge recorded downstream of the Project [*Hubbard et al.*, 1997], and its peak was captured by Round Butte Dam, whose reservoir was filling for the first time. For simplicity, we refer to the four storms that occurred after the filling of the reservoir as 'post-filling' events; all five events together are called 'post-dam' events.

Comparing hydrograph shapes for Project inflows and outflows showed that for all post-dam transport events, the Project stored water (inflow > outflow) on the rising limb of the hydrograph and released water (inflow < outflow) during and/or following the hydrograph peak (Figure 13). In all cases but the 1964 event, however, the amount of water stored and released was minimal compared to the overall discharge for the event and, in most cases, most changes in the hydrograph due to the Project occurred below critical discharge predicted for bedload transport. Although changes in the hydrograph at flows less than critical discharge are not important in the context of bedload transport or channel morphologic change, consequences of such flow reduction or enhancement on suspended sediment transport and ecological parameters might exist.

The Project had little effect on the magnitude or timing of post-filling-event flow peaks but delayed the peak of the 1964 event by four days and decreased its magnitude by around 140 m^3/s (Table 6). We consider the Project's effect on the 1964 event unique.

Using Project inflow and outflow discharge values for each post-dam transport event, the quantity of bedload transported per day by these flows was predicted and compared for Sites B and D. The results indicated that, at these sites, the Project slightly increased bedload transport for the four post-filling events and substantially decreased transport for the 1964 event (Table 7). Because Project inflows during the 1964 flood exceeded the upper limits of the sediment rating curve for Site B, transport rates for this event had to be extrapolated.

Channel Morphology

Comparison of USGS historical cross-section measurements for the Madras gage revealed that the channel bed was degrading at a very slow but statistically significant rate both prior to and following construction of the Project as indicated by decreasing minimum streambed elevations (2-sided p-value = 0.05 for 1924–1933; 2-sided p-value << 0.001 for 1929–1956 and 1957–1998) (Figure 14). Although absolute degradation rates between pre- and post-dam time periods cannot be compared because the measurement cross-section was moved when construction began on the Project in 1957, the slopes of the 1929–1957 and the 1957-1998 trend lines are similar. The largest decreases in minimum streambed elevation after 1957 appeared to be associated with high discharge events, particularly those exceeding the predicted critical discharge of 340 m^3/s (Figure 14b). Prior to 1957, the measurement cross-section was located in a boulder- and bedrock-controlled section (USGS, unpub-

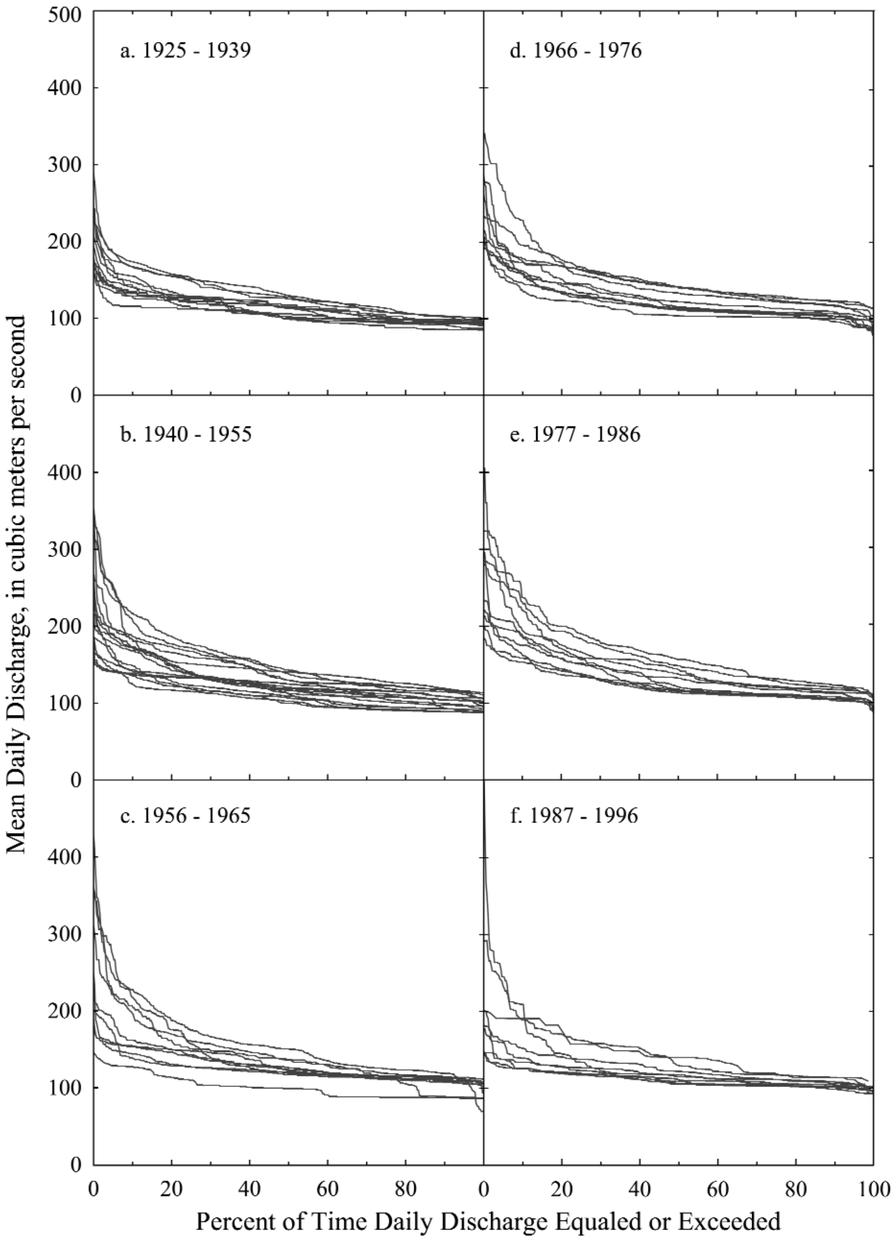

Figure 11. Annual flow duration curves (Deschutes River near Madras gage) for water years (a) 1925-1939, (b) 1940-1955, (c) 1956-1965, (d) 1966-1976, (e) 1977-1986, and (f) 1987-1996.

lished data, 1957) and, therefore, was not as affected by large flood events as the more alluvial post-1957 site (Figure 14). Between 1957 and 1998, net degradation at the channel thalweg was 0.14 m (Figure 14b). Average degradation of the thalweg over the same time period was 0.09 m (Figure 14b). For the post-1957 gage site, cross-sectional area was found to increase with time at a very small but statistically significant rate (2-sided p-value << 0.001), indicating a very slight increase in channel capacity over time (Figure 15). Pre-1957 areas were not calculated because of the extreme stability of the site (Figure 16).

Examination of individual cross sections before, during, and after high discharge events showed channel scour during the events and partial to total refilling of scoured areas

Table 5. Frequency and magnitude of critical discharge exceedance from 1924 to 1996 for calculated critical discharges of 270, 340, and 460 m^3/s.

Q_{cr} [a] (m^3/s)	# days $Q^b \geq Q_{cr}$	% of record $Q \geq Q_{cr}$	# days $Q>Q_{cr}$ by >10%	# days $Q>Q_{cr}$ by >20%
270	181	0.7	96	48
340	26	0.1	6	5
460	1	0.004	1	0

[a] Q_{cr} = critical discharge
[b] Q = discharge

in the following weeks to months (Figure 17). Maximum recorded scour at the Madras gage measurement cross-section was 0.8 m during the February 1996 flood (Figure 17e). Four months later, 0.5 m of the original 0.8 m scour had refilled (Figure 17e). The magnitude of channel "rebound" associated with high discharge events appears to be strongly related to the magnitude of the peak discharge experienced during the event (Figure 18). Similar channel rebound was noted much further downstream at the measurement cross-section for the 'Deschutes River at Moody' gage [*McClure*, 1998]

These empirical repeat cross-section surveys suggest that thresholds for general channel-bed entrainment at the Madras gage site are exceeded beginning around 250 m^3/s (Figure 17c, d, e). At this discharge and higher, the entire

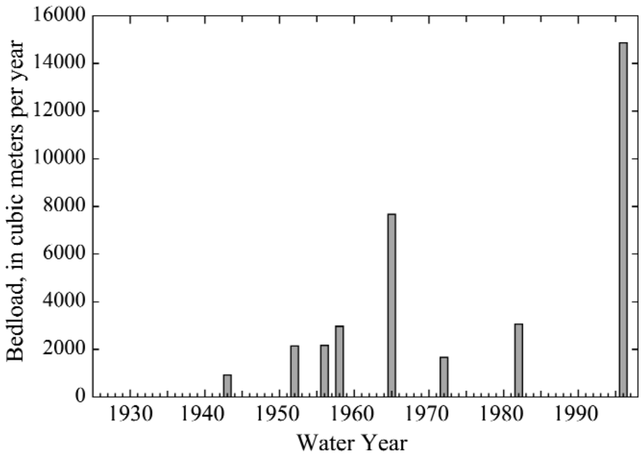

Figure 12. Predicted volume of bedload moved per year at Site B (RM 98.0) during water years 1925-1996.

cross section exhibited change. Channel change was concentrated in the thalweg for smaller discharges of about 150 m^3/s (Figure 17a, b). These results are generally in close agreement with the lower bound of critical thresholds predicted from the hydraulic models for both the cross-section average and the thalweg (Table 4).

Channel-bed Texture

Results from multiple regression analyses showed few or no significant longitudinal or temporal trends (Table 8). A modest decrease in armoring with distance from the dam was detected but otherwise no clear spatial or temporal trends in grain size emerged.

In the primary study reach, bed surface D_{50} values at island and bar heads ranged from 30 mm to 95 mm (average 70 mm) during 1995 and 1996 (Figure 19a). Results from multiple linear regression showed no significant evidence for a change in surface D_{50} with distance, even after accounting for year and abundance of *C. demersum* (Table 8). In addition, the Trask sorting coefficient showed very little difference in surface particle sorting between sites (Figure 19b). The coefficient generally ranged between 1.3 and 2.7, but reached 5.9 at the island at RM 88.3 in 1995. Better sorting within surface deposits was not observed close to the Project.

Spatial variations in grain size between sites were strongly influenced by abundance of *C. demersum*, which traps sand in an otherwise sand-poor bed. In particular, high levels of the macrophyte were strongly significant in lowering the median grain size in the primary study reach (p-value = 0.006; extra sum of squares F-test) (Table 8). The four lowest D_{50} values represented two sites (islands at RM 88.3 and RM 98.9, Figure 19a) where macrophyte levels were especially high in both 1995 and 1996.

There was also little change in surface grain-size as a whole, between years at each site (Figure 20a). Even after accounting for the effects of *C. demersum*, there was no statistical evidence for an overall change in surface D_{50} following the 1996 flood (Table 8).

The bed subsurface D_{50} in the primary study reach was finer than that of the surface and ranged from 5 mm to 50 mm (average 20 mm, Figure 20b). The final statistical model showed no evidence for a longitudinal trend in subsurface D_{50} values when year and the abundance of macrophytes were accounted for in the primary study reach (Table 8).

The final statistical model showed no significant evidence for a temporal change in subsurface D_{50} in the primary study reach (Table 8). The data point representing the bar at RM 89.6 was influential in the regression, however. When

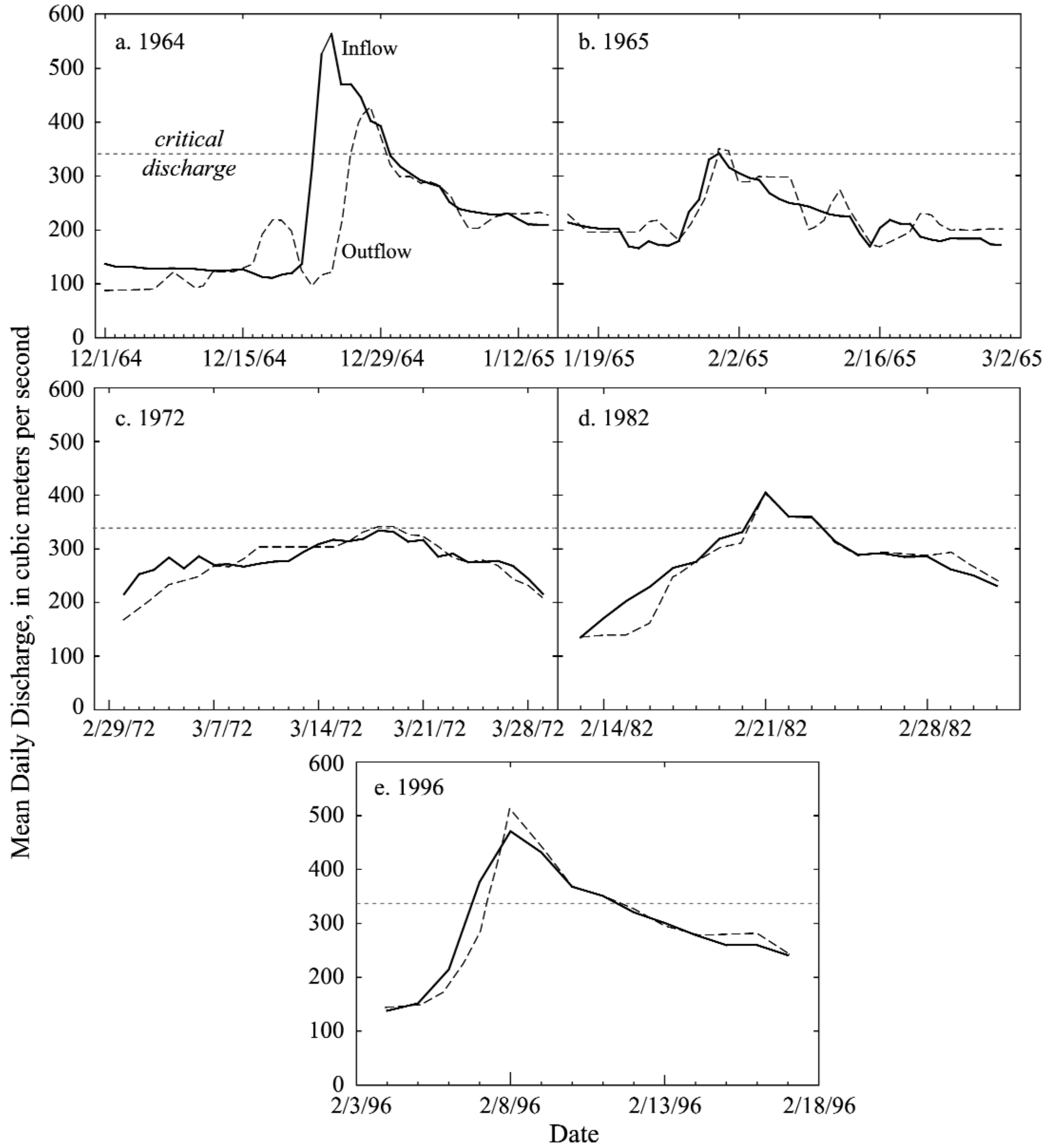

Figure 13. Lake Billy Chinook inflows and Project outflows for all post-dam transport events: (a) December 1964, (b) January 1965, (c) March 1972, (d) February 1982, (e) and February 1996.

removed from the analysis for comparison, the overall decrease in subsurface D_{50} between years was significant (2-sided p-value = 0.012), suggesting that the subsurface may have fined somewhat in response to fine sediment inputs during the flood of February 1996.

Armoring ratios ranged from 1.3 to 11.9 (average 4.0) and generally declined with distance from the Project (Figure 20c). Multiple linear regression showed that the longitudinal trend in armoring was statistically significant (Table 8). The mean armoring ratio was estimated to be 0.16 less with each kilometer from the Project (95% confidence interval between 0.013 and 0.30). Although not statistically significant at p = 0.05, the results indicated that there might also have been an increase in armoring following the February 1996 flood (Table 8). Three of the four sites closest to the Project showed the largest increases in armoring between years (Figure 20c). Data points from 1996 representing the bar at RM 99.6 and the island at RM 98.1 were influential in

Table 6. Timing and magnitude of highest flow peaks for reservoir inflows (Q_{in}) and outflows (Q_{out}) for post-dam transport events. All discharges are mean daily flow.

Transport Event	Magnitude of Highest Flow			Date of Highest Flow		
	Q_{in} (m^3/s)	Q_{out} (m^3/s)	% change	Q_{in}	Q_{out}	Days peak lagged
December 1964	564[a]	428	-32	24 Dec. 1964	28 Dec. 1964	4
January 1965	341[a]	348	2	31 Jan. 1965	31 Jan.1965	0
March 1972	334	343	3	18 Mar. 1972	18-19 Mar. 1972	0
February 1982	405	405	0	21 Feb. 1982	21 Feb. 1982	0
February 1996	471	510	8	8 Feb. 1996	8 Feb. 1996	0

[a] Estimated value due to lack of reservoir water elevation data

Table 7. Total bedload transported by reservoir inflows ($Q_{s\ in}$) and outflows ($Q_{s\ out}$) for five post-dam transport events. Reservoir inflows approximate streamflows that would occur in the absence of the Project. Transport calculations for Site D (except in 1996) do not take into account the discharge contributed by Shitike Creek as the creek was not gaged at this time.

Site	Transport Event	$Q_{s\ in}$ (m^3)	$Q_{s\ out}$ (m^3)	% change in $Q_{s\ in}$
B	December 1964	48,000	6,526	-86
D	December 1964	13,900	4,301	-69
B	January 1965	1,100	1,200	9
D	January 1965	1,400	1,600	14
B	March 1972	0	1,700	--
D	March 1972	0	1,900	--
B	February 1982	3,100	3,100	0
D	February 1982	3,000	3,100	3
B	February 1996	11,700	14,900	27
D	February 1996	9,700	10,400	7

this regression. When the two points were removed separately or in combination, the decrease in armoring with distance from the Project remained significant at the 0.05 level. In two of these scenarios, there was strong evidence for an increase in armoring between 1995 and 1996. However, when only the point from the island at RM 98.1 in 1996 was removed, the temporal change was not significant at even the 0.1 level. Thus, the model was greatly influenced by these points and the increase in armoring with time cannot be shown conclusively.

Multiple linear regression models constructed for the entire study area showed no significant evidence for a longitudinal trend in surface D_{50}, subsurface D_{50}, or armoring (Table 8, Figure 21). In addition, the Trask sorting coefficient showed very little difference in surface particle sorting between sites over the entire study reach (Figure 22). Thus, bed coarsening or greater sorting was not observed in the primary study reach relative to the lowermost 140 km of the river.

Tributary D_{50} values were generally finer than mainstem values. Of the sampled tributaries, only the Warm Springs River had a coarser grain-size distribution than the mainstem (Figure 23). Grain-size distributions from tributaries generally exhibited similar sorting compared with the mainstem surface bed material.

Most grain-size distributions from the fourteen sampled tributaries were remarkably similar to each other (Figure 23), with D_{50} values averaging 50 mm (range 10–105 mm) and Trask sorting coefficients averaging 2.4 (range 1.4–11.6). However, the two largest tributaries, the Warm Springs and White Rivers, did have particularly distinct grain-size distributions. The White River showed a strongly bimodal distribution, with a high proportion of material

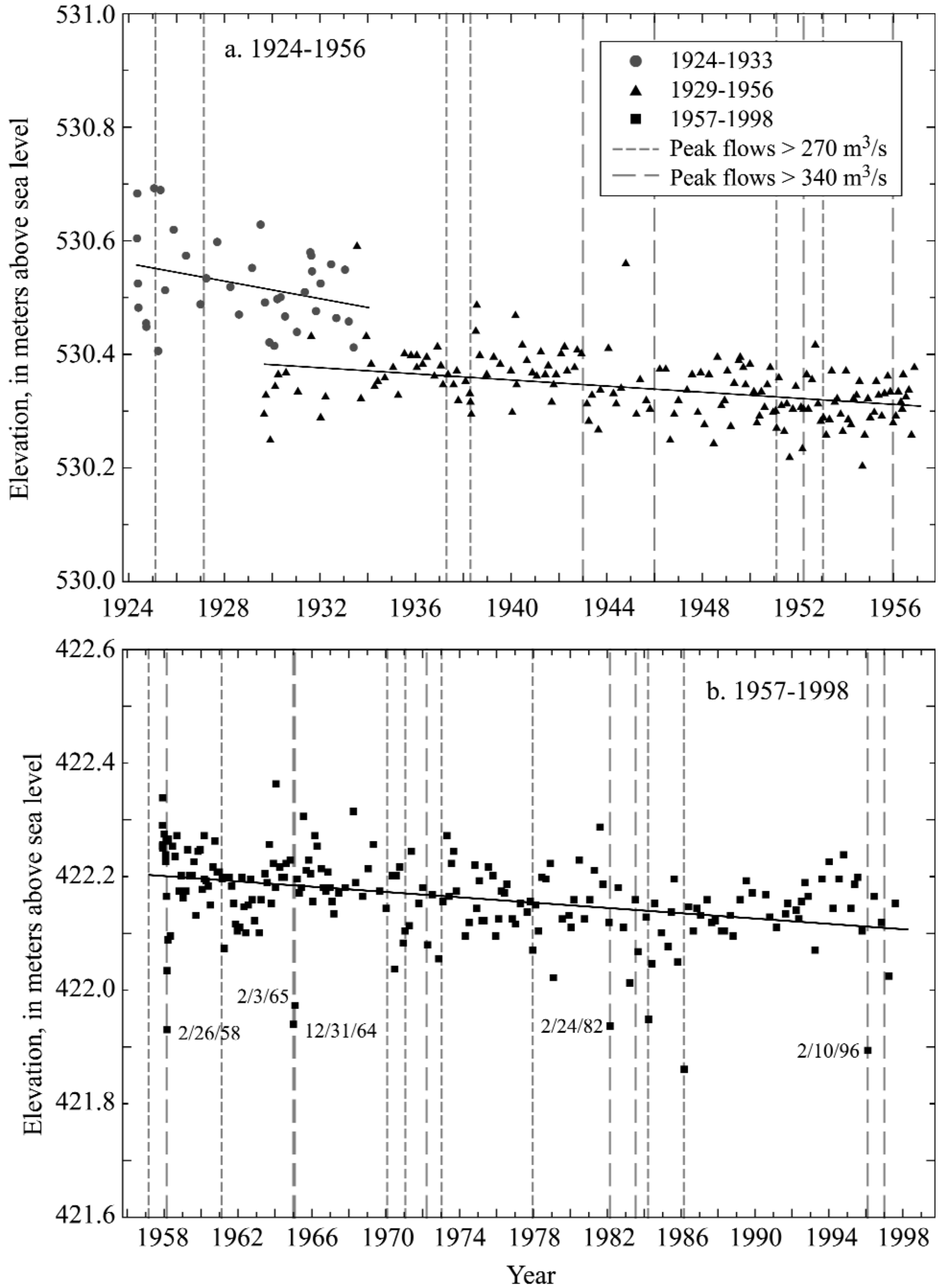

Figure 14. Minimum streambed elevations (i.e., elevation of channel thalweg) of USGS measurement cross-section for the Deschutes River near Madras gage, (a) 1924-1956 and (b) 1957-1998.

less than 2 mm in diameter (Figure 23), presumably sandy material derived from reworked lahar and glacial deposits from Mt. Hood. There was no apparent decrease in D_{50} values in the mainstem Deschutes directly downstream of the White River confluence, however (Figure 24). The Warm Springs River had a relatively coarse grain-size distribution (Figure 23). Despite this, mainstem D_{50} values registered no coarsening downstream of the Warm Springs River confluence (Figure 24). Thus, even where tributaries input the most distinctive bed material to the mainstem, noticeable shifts in the mainstem bed material size did not occur.

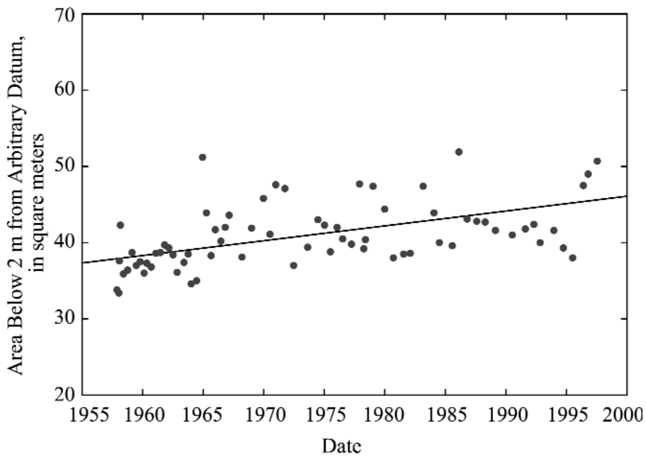

Figure 15. Area of USGS measurement cross-section below 2 meters from arbitrary datum (Deschutes River near Madras gage).

DISCUSSION

Our analyses of bedload transport, channel morphology, and channel-bed texture all consistently characterize the Deschutes River as an unusually stable alluvial river. That stability is reflected in the infrequency of bedload transport events both prior to and following dam construction, the absence of pronounced morphologic or textural change following the record flood in February 1996, and the uniformity of grain size along the channel. Here we consider in detail some aspects of the Deschutes' stability and discuss its causes and implications for assessing the effects of the Project.

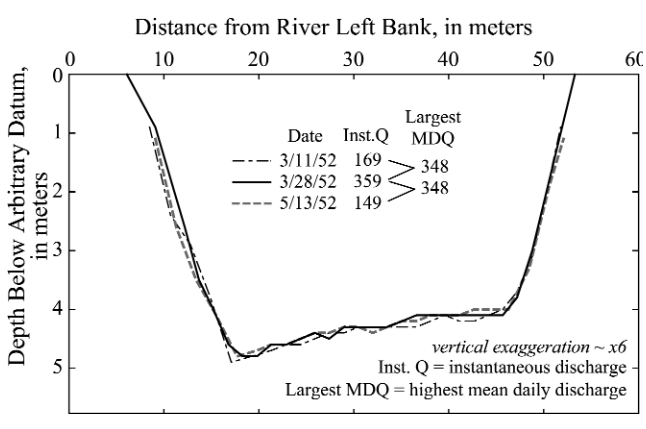

Figure 16. Cross-sectional profiles at the USGS measurement cross-section for the Deschutes River near Madras gage before, during, and after a large flood in March 1952.

Evidence for Channel Stability

Frequency and Magnitude of Bedload Transport. Modeled estimates of critical discharge were generally consistent across sites (Table 4), giving confidence in results of the hydraulic model. General mobility of the channel bed was predicted to begin at discharges of around 340 m^3/s or, incorporating the results of the sensitivity analysis, between 270 and 460 m^3/s for primary study reach sites. These model results were evaluated against a detailed analysis of long-term cross-section change in relation to discharge. The cross-section analysis (1957–1998) showed general mobility of the channel bed beginning around 250 m^3/s, near the lower end of the predicted range (Figure 17). Furthermore, the dates during which bedload transport was predicted to occur (post-1957) coincide with the lowest measured elevations of the channel thalweg at the USGS measurement cross-section (Figure 14), indicating that channel scour did occur during these events, as predicted.

Bedload transport at sites in the primary study reach was predicted to occur less than 1% of the time from 1924 to 1996. The combined effects of reasonable uncertainties of parameters used in the hydraulic modeling did not substantially alter these results. This frequency of transport is much lower than that in other gravel-bed rivers where studies have shown that bed material is typically moved about 5–10% of the time, or several times per year, at flows close to bankfull [*Andrews and Nankervis*, 1995]. The extremely low frequency of bedload transport in the Deschutes River appears to result from the very uniform flow regime, absence of high flows, and coarse gravel-to-cobble substrate with a relatively high entrainment threshold.

The volume of bed material moved was also predicted to be low, generally between 2,000 and 3,000 m^3/year for years in which transport occurred (Figure 12). In comparison, the Kemano River in British Columbia, Canada, a river with similar discharge and particle size to the Deschutes, has an estimated mean annual bedload transport rate of about 50,000 m^3/year [*Church*, 1995]. During water year 1996, the most active year on record, the Deschutes was predicted to have moved only around 15,000 m^3 of bed material (Figure 12, Table 7).

Low predicted frequency and magnitude of bedload transport and no physical evidence for channel aggradation implies that the lower Deschutes River has historically been a sediment-poor system both prior to and following Project construction. This inference is supported by a calculation of sediment discharge rates into Round Butte Reservoir [*O'Connor, Grant and Haluska*, this volume]. Results from a sedimentation survey of this reservoir indicated that about

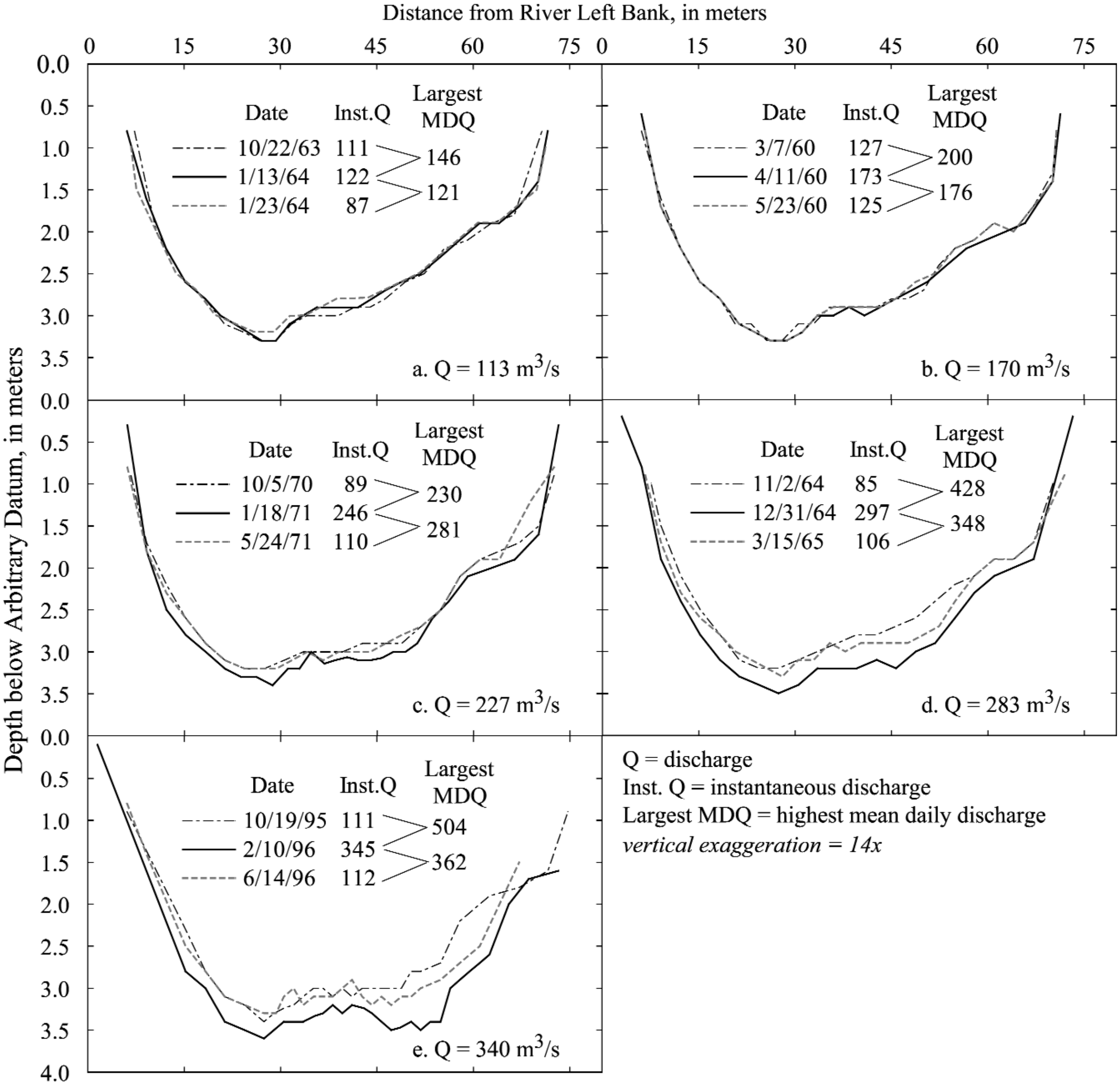

Figure 17. Cross-sectional profiles at the USGS measurement cross-section for the Deschutes River near Madras gage showing degree of bed response for flow events of different sizes.

1,249,000 m^3 of sediment had been captured by Round Butte Dam between 1964 and 1998. This volume is nearly all the sediment of all particle sizes input from the Crooked and Deschutes Rivers to the mainstem lower Deschutes over 34 years. The Metolius River fan was smaller than the detection limits of the survey. Using a sediment density of 2,740 kg/m^3 [*Fassnacht*, 1998], the effective unit sediment supply rate was calculated to be about 11 $tonnes/km^2yr$ for the 9,740 km^2 drainage basin above Round Butte Dam that directly contributes sediment (J.E. O'Connor, USGS, unpublished data, 1999). This is an extremely low sediment supply rate relative to other rivers (Table 9).

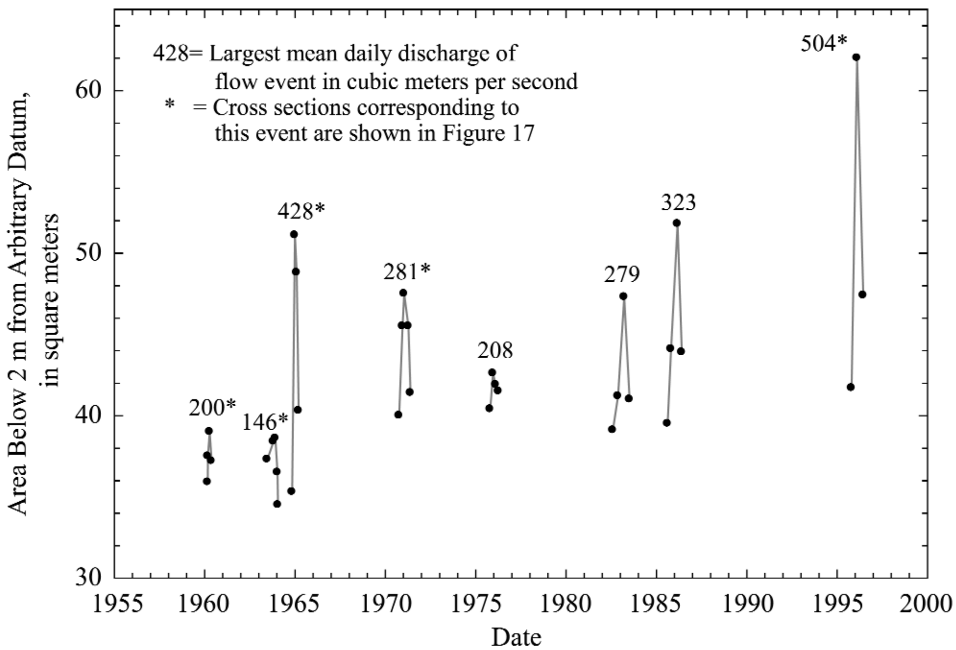

Figure 18. Channel rebound associated with high discharge events, Deschutes River near Madras measurement cross-section 1966-1996.

These recent sediment surveys provide additional support to model predictions of low frequency and magnitude of bedload transport. If sediment supply is low and model predictions were incorrect (that is, if frequency and magnitude of transport were high), we would expect high rates of channel degradation and/or high armoring ratios directly downstream of the Project. Degradation rates just below the Project are about 2.2 mm/year both before *and* after dam closure (Figure 14). This rate of degradation is very low in comparison to those below dams from other selected U.S. rivers (Table 10). Results from the channel-bed textural analysis also did not show any trends in armoring downstream of the Project (Figure 21).

The effects of the flood of February 1996, with the highest recorded peak discharge, provide additional support for interpretations of channel stability. This flood was predicted to have produced transport rates much larger than those from any other recorded event on the Deschutes River. Subsequent field investigations in April, August, and September 1996, indicated that bedload transport did occur during the flood as predicted by the hydraulic and bedload transport modeling. Field evidence of transport included the presence of new gravel and cobble deposits both in-stream and on vegetated islands and floodplains, and the absence of former small islands in the lower river. Although the flood resulted in localized bedload transport and disturbance of vegetation, it did not substantially reorganize channel bars and other surfaces; its most visible effect was the uprooting and breakage of riparian vegetation.

The occurrence of this large flood during the study period allowed us to examine whether the limited geomorphic change in the Deschutes was related to erosion thresholds not being exceeded since Project construction. Coarse-bedded rivers elsewhere have been shown to experience little or no degradation following impoundment because of the general infrequency of mobilizing flows [*Petts*, 1979; *Church*, 1995]. *Petts* [1979] hypothesized that in such ‘non-mobile channels’ a rare large flood, crossing some intrinsic threshold, may be required before channel adjustments will begin. Once that geomorphic threshold has been exceeded, a rapid phase of adjustment might ensue, redistributing channel and floodplain sediments. Critical discharge calculations predicted initiation of bedload transport at a discharge of about 340 m^3/s as measured at the Madras gage. The flood of 1996 had a maximum mean daily flow of about 510 m^3/s at the Madras gage. Despite its slightly less than 100-year return interval [*Hosman et al.*, this volume], the 1996 flood did not appear to be the kind of large resetting flood *Petts* [1979] discussed, as it had little effect on the existing bars and islands. Larger and more infrequent events are apparently

Table 8. Summary of regression results for the Primary Study Reach and lower river. Models shown below table.

	Surface D_{50} (mm)		Subsurface D_{50} (mm)		Armoring ratio (mm/mm)	
Independent variables	Value of β Coefficient	2-sided p-value	Value of β Coefficient	2-sided p-value	Value of β Coefficient	2-sided p-value
Primary Study Reach						
Constant (Low *C. dem.*, 1995)	-34.30	0.68	110.74	0.044[a]	-21.00	0.062
River Kilometer	0.73	0.19	-0.56	0.11	0.16	0.034[a]
YEAR (0 for 1995, 1 for 1996)	6.53	0.32	-6.54	0.14	1.68	0.07
C. demersum: (1 for moderate)	1.54	0.84	n/a[b]	n/a	n/a	n/a
C. demersum: (1 for high)	-28.12	0.0052[a]	n/a	n/a	n/a	n/a
Entire Study Area						
Constant	87.68	<0.0001[a]	30.14	0.0003[a]	2.59	0.07
River Kilometer	-0.13	0.23	-0.08	0.14	0.02	0.14

[a] Statistically significant (<0.05) p-values
[b] n/a = not applicable

Models used:

Primary Study Reach: $|\mu(\text{surface } D_{50})| = \beta_0 + \beta_1(RK) + \beta_2(YEAR) + \beta_3(CD) + \beta_4(CD)$; $|\mu(\text{subsurface } D_{50})| = \beta_0 + \beta_1(RK) + \beta_2(YEAR)$; $|\mu(\text{armor})| = \beta_0 + \beta_1(RK) + \beta_2(YEAR)$

Entire Study Area: $|\mu(\text{surface } D_{50})| = \beta_0 + \beta_1(RK)$; $|\mu(\text{subsurface } D_{50})| = \beta_0 + \beta_1(RK)$; $|\mu(\text{armor})| = \beta_0 + \beta_1(RK)$

where μ = the estimated mean of the grain parameter indicated, RK = River Kilometer, $YEAR$ = year, CD = the level of *C. demersum*, and β values represent coefficients in each regression model (β_0 = y intercept or D_{50} when all other β values equal zero, β_1 = RK, β_2 = 0 for 1995, β_2 = 1 for 1996, β_3 = 1 for moderate levels of *C. demersum*, β_4 = 1 for high levels of *C. demersum*).

responsible for shaping the primary channel features and morphology of the lower Deschutes River.

Channel Features, Vegetation Patterns, and Historical Channel Changes. Channel morphological features and vegetation patterns along the lower Deschutes River and the results of the analysis of historical channel changes all support the interpretation of general channel stability. The river contains very few meander bends and point bars—common features in active alluvial channels. Many of the existing meanders are deeply incised into the lava flows that comprise the steep canyon walls. Tributary fans have built out into the river and constrained the channel. These fans appear to be old, judging from the age of their vegetation and their heavily weathered and desert-varnished boulders, and from the observation that the fans were not substantially modified by the February 1996 flood.

Channel stability is also implied by the scarcity of unvegetated deposits in the river. Islands, tributary fans, and floodplains are covered with grasses, sagebrush (*Artemesia spp.*), willows, sedges, and alders. Alders around 20+ years old can be found lining long stretches of channel banks and along the edges of many islands. These would be unlikely features if the Deschutes were an active alluvial river in which cobble, gravel, and sand deposits were often reworked. Aerial photographs also show stable channel boundaries and island locations [*Curran and O'Connor*, this volume]. Changes that do occur in island and bar morphology following floods tend to be associated with tributary confluences. One of the few islands that is not heavily vegetated is the first island downstream of the Shitike Creek confluence. New gravel was deposited on top and along the sides of this island by the February 1996 flood.

Analyses of historical cross-sections also suggest general channel stability. USGS cross-section measurements for the Madras gage showed extremely limited channel-bed degradation over the period of record (Figures 14, 16, 17). Lateral movement of the channel at the cross-section was minimal (Figures 16, 17). The majority of channel scour noted dur-

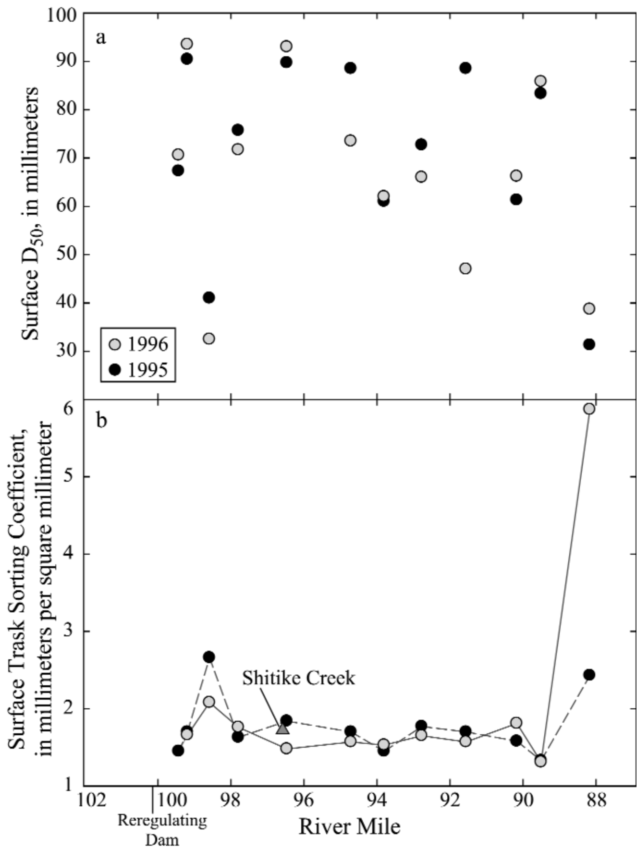

Figure 19. Grain-size data for bar and island heads in the primary study reach in 1995 and 1996: (a) Surface D_{50} values; (b) Trask sorting coefficients for surface bed-material.

ing high flow events was refilled in the weeks to months following the event (Figures 17, 18), indicating a state of relative balance between these opposing processes acting on the channel perimeter.

Project Effects on the Geomorphology of the Lower Deschutes River

The results of the bedload transport, channel morphology, and channel-bed texture components of our study provide strong evidence for the intrinsic stability of the Deschutes River system. Within this context of a stable channel environment, we now evaluate the direct effects of the Project on the lower Deschutes River.

Streamflow and Bedload Transport. The low frequency of discharges surpassing the predicted threshold for bedload transport provides a small data set with which to evaluate the downstream effects of the Project on bedload transport frequency and magnitude. Only four transport events were predicted to have occurred during the 30+ years since Round Butte Reservoir was filled. A single high flow event can greatly affect the calculated frequency and magnitude of transport for a given time period (pre- or post-Project). Despite this, our results did not indicate any major natural or anthropogenic changes in the frequency and magnitude of either discharge (Figures 2, 11) or of bedload transport (Figure 12) in the primary study reach following Project construction. Examination of individual events following Project construction did, however, suggest more subtle changes in both discharge and bedload transport at the event scale (Figure 13, Tables 6, 7). Low frequency and magnitude of bedload transport, low sediment supply, and minimal Project-induced effects on streamflow suggest only limited channel degradation, or morphological or textural change, should be expected in the primary study reach following impoundment. Results of the historical cross-section and channel-bed texture analyses support this conclusion (Figures 14-18, 21).

Channel-bed Texture. No clear longitudinal trend in the surface and subsurface bed-material size distribution emerged in either the primary study reach or entire study area. Data points obtained from the same sites for different years are generally similar to each other; for this reason, finding no longitudinal pattern in surface D_{50} values cannot be attributed to sampling error. Modeling results suggest that downstream distance and year do not significantly influence bed material properties.

The marked uniformity of grain sizes and armoring over the entire course of the river below the dams reflects absence of major changes in channel slope, limited range of grain sizes introduced as bedload by tributaries, and minor hillslope inputs from bedrock canyon walls. No clear differences in grain size were noted upstream and downstream of major tributaries, where changes in longitudinal grain-size distribution patterns due to partially replenished sediment supply might be expected (Figure 24). Several factors account for this longitudinal uniformity: high transport efficiency of fine sediment by the mainstem, opportunities for storage of tributary sediment in alluvial fans at tributary junctions, and similarity of bed-material size ranges between the main channel and tributaries. For example, much of the material transported by the White River during high flow events may be suspended sediment [*U.S. Department of Energy*, 1985], which is easily transported out of the basin by the Deschutes. As a result, the bed of the Deschutes is not noticeably finer downstream of the White River (Figure 24). Coarser bed materials carried by the Warm Springs River are typically deposited within the extensive, coarse fan complex at its confluence with the

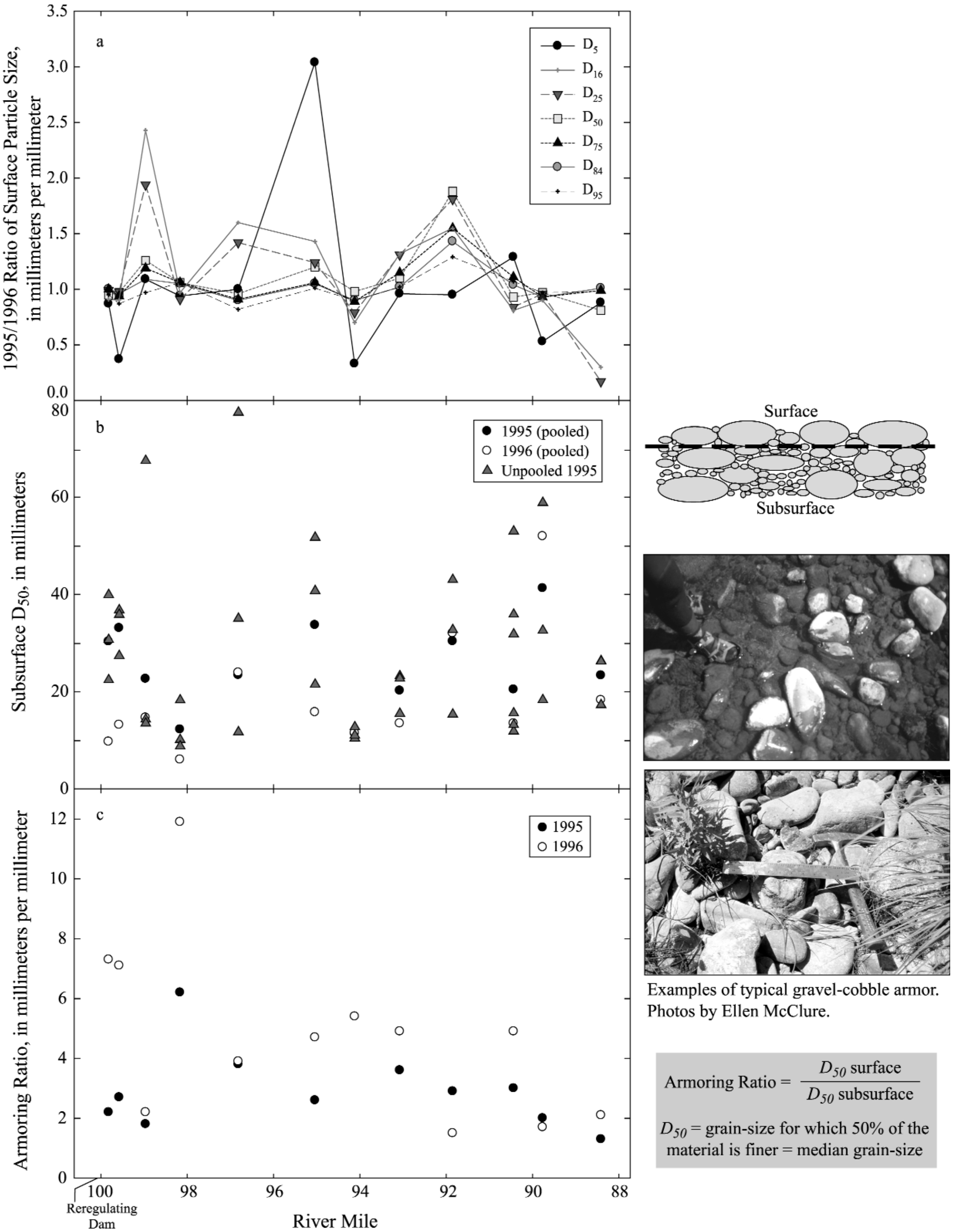

Figure 20. Grain-size data for bar and island heads in the primary study reach: (a) Surface grain-size distribution ratios $D_{x(1995)}/D_{x(1996)}$; (b) Subsurface D_{50} values; (c) Armoring ratios for 1995 and 1996.

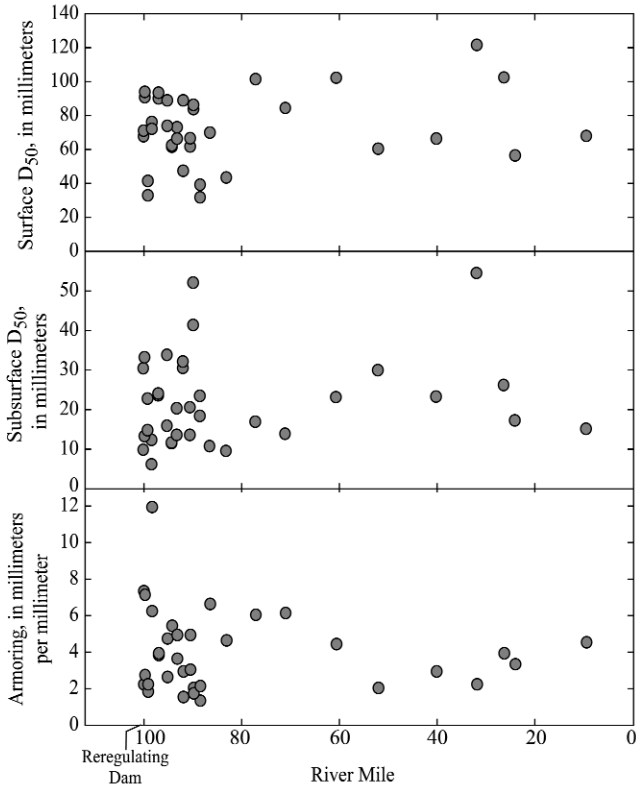

Figure 21. Surface D_{50} values, subsurface D_{50} values, and armoring ratios for bar and island heads along the entire study area in 1996. Note that scales are different for each plot.

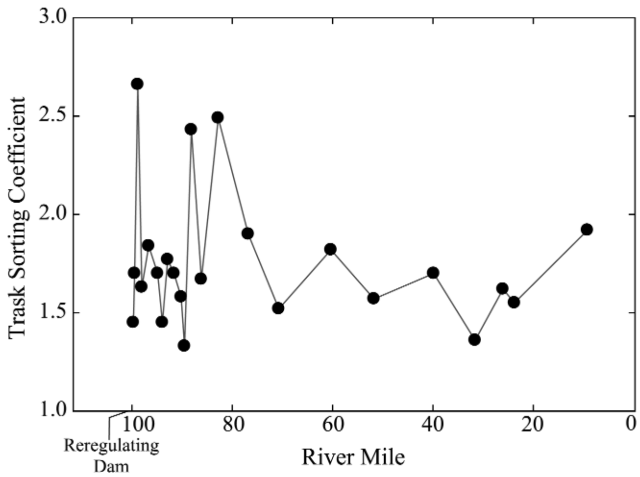

Figure 22. Trask sorting coefficients for surface bed-material at bar and island heads along entire study area in 1996.

Deschutes. Sediment derived from the White and Warm Springs Rivers represents material with the largest size deviations from that of the mainstem, but for the most part is not incorporated into mainstem bed material (Figure 24). Some inputs of gravel from Shitike Creek, whose bed material more closely resembles that of the mainstem, appear to be deposited locally within the mainstem, inducing local, minor morphologic changes (for instance, island growth) and textural shifts in the channel bed.

High armoring ratios near the Project (up to 11.9 at RM 98.1) after the 1996 flood appear to have resulted from subsurface fining, as the surface layer did not change significantly between years. This apparent increase in armoring via subsurface fining is contrary to most models of armor development [i.e., *Parker et al.*, 1982; *Dietrich et al.*, 1989]. If sediment supply below the Project were substantially reduced, one would expect selective erosion to cause downstream winnowing of bed material. This would cause the surface grain-size to coarsen with time near the Project and for the coarsening front to prograde downstream, particularly during high flow events. Such changes were not observed. Erosion of channel banks and islands by floodwaters may have introduced fine material into the sediment load, although no apparent or adequate source of fine sediment exists in this reach. Fine sediment from sources upstream of Pelton Dam (i.e., Seekseequa Creek; Figure 1) may have contributed fine material to downstream sample sites through turbid water releases from the Project during the February 1996 flood. The flood caused several large headcuts, and substantial erosion and sediment transport out of Seekseequa Creek into the reservoir behind Pelton Dam (C. Gannon, Confederated Tribes of Warm Springs, oral communication, 1999). Consequently, the three high armoring ratios measured near the Project may not be correlated with the Project itself.

Another possible explanation for the apparent fining of subsurface bed-material between years is that subsurface sample sizes were smaller than necessary for accurately distinguishing temporal changes. While good precision in the sample mean can be achieved with sample sizes less than those suggested by *DeVries* [1970] and *Church et al.* [1987] for moderately sorted material, the accuracy is much less certain for smaller samples of poorly sorted materials such as fluvial gravel [*Ferguson and Paola,* 1997]. Following the criteria of Church et al. [1987], the requisite size of a representative bulk sample of channel-bed subsurface material may be estimated by the largest particles in the surface population, as long as the surface constitutes the same deposit. Using the average surface D_{95} value of 150 mm for sites in the primary study reach, the proposed 0.1% of sample size

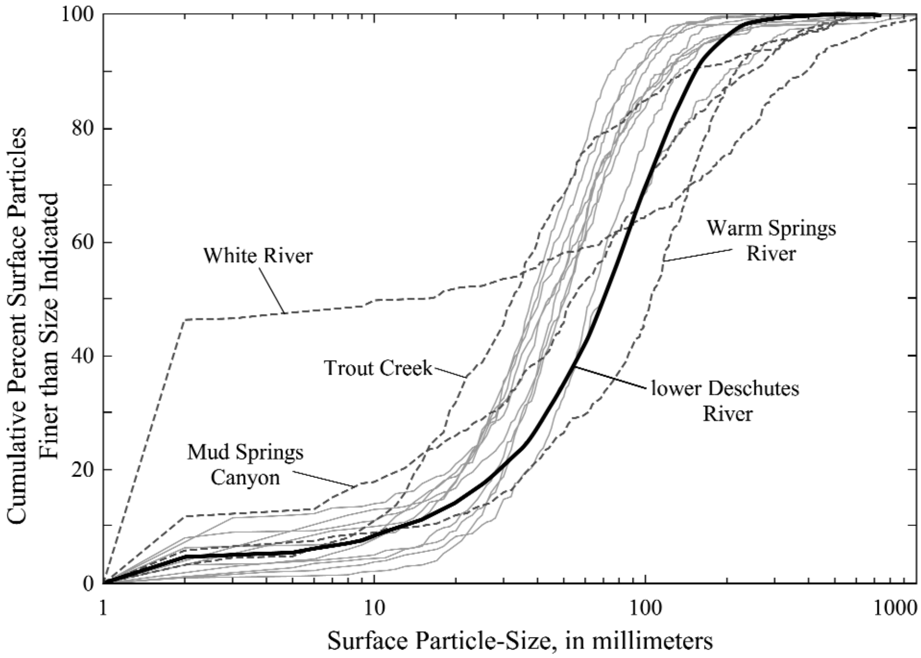

Figure 23. Surface grain-size distributions of fourteen sampled tributaries of the lower Deschutes River.

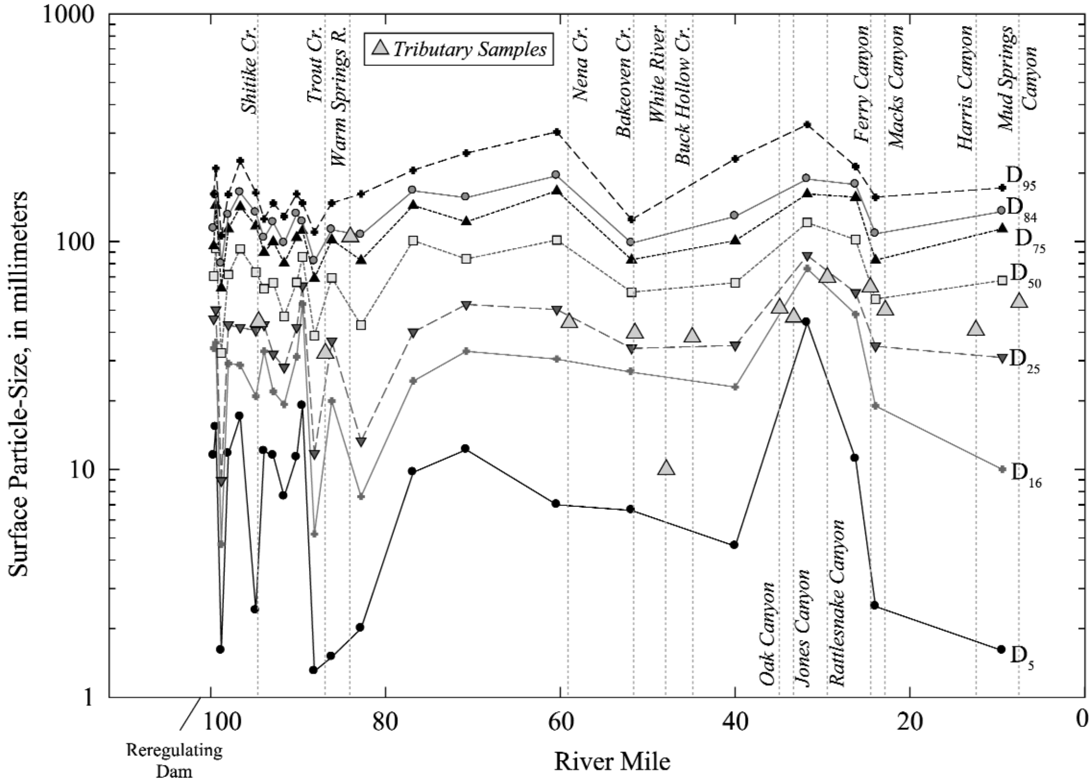

Figure 24. Surface grain-size percentiles of sample sites over the entire study area in 1996 relative to those of tributary confluences.

Table 9. Sediment discharges for selected North American rivers.

		Drainage Area (10^6 km^2)			Sediment Discharge (10^6 t/yr)			Unit Sediment Discharge (t/km^2/yr)		
River, Country	Location	*Judson & Ritter* [1964]	*Milliman & Meade* [1983][a]	*This paper*	*Judson & Ritter* [1964]	*Milliman & Meade* [1983][a]	*This paper*	*Judson & Ritter* [1964]	*Milliman & Meade* [1983][ab]	*This paper*
Eel, USA	Scotia, California	0.0081	0.008	…	16	14	…	2048	1750	…
Mad, USA	Arcata, California	0.0013	…	…	2	…	…	1300	…	…
Trinity, USA	Hoopa, California	0.0073	…	…	3	…	…	400	…	…
Snake, USA	Central Ferry, Washington	0.27	…	…	12	…	…	44	…	…
Columbia, USA	Pasco, Washington	0.27	0.67	…	9	8	…	35	12	…
Green, USA	Palmer, Washington	0.0006	…	…	0.06	…	…	108	…	…
Fraser, Canada		…	0.22	…	…	20	…	…	91	…
Yukon, USA		…	0.84	…	…	60	…	…	71	…
Copper, USA		…	0.06	…	…	70	…	…	1167	…
Deschutes, USA	Madras, Oregon	…	…	0.0095	…	…	0.10	…	…	11

[a] Location not provided for these data.
[b] Unit sediment discharge calculated here from data derived from *Milliman and Meade* [1983].

Table 10. Channel-bed degradation rates below dams for selected U.S. rivers[a].

						Total Change in Mean Bed Elevation			
River, Dam, State	Year Dam Closed	Reference Year[b]	Last Year of Data Evaluated	# Dates[c] for which Data Evaluated	Cross-section Distance from Dam (km)	Range for Years Evaluated (m)	Mean (m)	Standard Deviation (m)	Average Rate of Channel Elevation Change (mm/yr)
Arkansas, John Martin, Colorado	1942	1943	1972	3	3.5	-0.10 to –1.95	-0.82	0.99	-27
Missouri, Fort Peck, Montana	1937	1936	1973	7	9.2	-0.65 to –0.90	-0.74	0.09	-20
Medicine Cr., Medicine Creek, Nebraska	1949	1950	1977	5	0.8	-0.10 to –0.20	-0.18	0.04	-6.4
Smoky Hill, Kanopolis, Kansas	1948	1946	1971	4	0.8	-0.80 to –1.45	-1.16	0.28	-51
Middle Loup, Milburn, Nebraska	1955	1950	1971	13	0.2	-0.60 to 2.65	-1.88	0.58	-115
North Canadian, Canton, Oklahoma	1948	1947	1976	6	1.8	-0.90 to 3.00	-2.05	0.94	-73
Red, Denison, Oklahoma-Texas	1942	1942	1969	4	0.6	-1.25 to –1.60	-1.41	0.15	-52
Deschutes, Pelton-Round Butte, Oregon	1956[d]	1957	1998	211	0.1	0.12 to –0.33	-0.06	0.06	-1.4
channel thalweg only						*0.15 to –0.39*	-0.09	*0.08*	*-2.2*

[a] Data used in calculations obtained from Table 13, *Williams and Wolman* [1984], except data presented for the Deschutes River.
[b] For this year, total change of channel bed is shown as 0 m, and therefore, acts as a reference point for later measurements.
[c] Not including reference year.
[d] Round Butte Dam closed 1962, see Table 2, this paper.

for the largest clast would then require a sample weighing about 5,000 kg per site. Even using a relaxed criterion of 5% would still require 100 kg of bed material. Because of the potential error resulting from sample size, there is no evidence for subsurface fining, and consequently an increase in armoring, between years. The substantial labor involved in transporting such large sediment samples from a wilderness river and laboratory time required to process such samples is daunting. A precise description of grain-size distributions of bulk samples remains a difficult problem in studies of gravel-bedded rivers.

Geomorphic Implications of Channel Stability

Within the context of downstream response of a channel to river regulation, there are at least two implications of a stable river. First, a stable river might be able to withstand a relatively wide range of changes in flow with little effect on channel morphology and bed texture because the channel bed, for the most part, remains immobile. This may represent the current situation for the lower Deschutes River, where most changes in streamflow occur at discharges that are less than critical (Figure 13). Even relatively large flows, such as those that occurred in February 1996, are unable to rework the channel substantially, perhaps because of the very low volume of sediment available for transport.

The second implication is that the imprint and consequences of whatever changes *do* occur in the channel may persist for a very long time. For example, if reservoir operations further reduced the already infrequent occurrence of flows near the threshold for bed material transport, textural changes such as increased compaction, cementation, or cohesion of bed materials could result, further reducing bed mobility. Here, not having a disturbance event can be a disturbance event itself [*Junk et al.*, 1989]. On the other hand, changes to the channel morphology induced by surpassing high geomorphic thresholds, such as appears to have occurred during rare and exceptionally large paleofloods, could persist for geologically long periods of time until the next high magnitude disturbance event. Field evidence suggests that, during the Pleistocene and Holocene, mechanisms existed for generating floods much larger than anything recorded over the last seventy-plus years [*Beebee and O'Connor*, this volume; *O'Connor et al.*, this volume]. These mechanisms included outburst floods from large landslide dams, debris flows, and glacially dammed lakes [*O'Connor et al.*, this volume]. The legacy of these floods persists in the major rapids and slope profile breaks at Whitehorse, Buckskin Mary, and Boxcar (Figure 8) [*O'Connor et al.*, this volume], all of which were only slightly modified by the 1996 flood.

It was hypothesized that historically low sediment supply to and transport rates in the Deschutes River would limit textural and morphologic adjustments of the lower river following impoundment. Our results strongly support an inference of low rates of sediment supply and bedload transport. They also confirm very limited textural and morphologic change. The minor hydrological changes noted in the flow record since regulation suggest little change in the frequency of bed-mobilizing flows, and the results of the historical cross-section analysis show no change in the trend of minor channel-bed degradation that preceded Project construction. In other words, both the ratio of post- to pre-Project frequency of mobilizing flows and the ratio of post- to pre-Project sediment supply may be close to 1. In this case, morphologic and textural response downstream from the Project should, for the most part, be small. While it is possible that the morphological manifestations of a reduced sediment supply (i.e., degradation and coarsening of the channel bed) due to gravel being trapped behind the Project have not had a chance to occur, very modest change over the thirty-plus year Project history, which includes some major storms, argues against dramatic changes in the near future.

CONCLUSIONS

Independent analyses of hydraulics and bedload transport, historical streamflow, morphologic change, and channel-bed texture together present a convincing argument that the Pelton-Round Butte Hydroelectric Project has done little to alter the lower Deschutes River's naturally low frequency and magnitude of bedload transport. In a system with low sediment supply, this has resulted in little apparent morphologic or textural response downstream of the Project. The river downstream of the Project appears to be astonishingly stable within its current flow regime and sediment supply, with the low rates of sediment transport keeping pace with the modest inputs of sediment. In a larger context, this study suggests that armoring, degradation, and morphologic change below dams may be limited where sediment transport rates and sediment supply are low.

Many studies of other rivers document armoring and degradation of the channel bed due to reduced sediment supply where flows are still competent to move a large portion of the bed material. In contrast, the Deschutes River represents a unique hydrologic and sedimentologic environment where sediment supply and transport may be limited within time scales defined by the historical flow record.

Acknowledgements. The authors gratefully acknowledge the many people who aided in logistics, field work, and/or field data collection, including Don Ratliff (PGE), Chris Zimmerman (Oregon State University), Scott McCollister (PGE), Eric Schulz (PGE), Tom Herrett (USGS), Tony Sorano (USGS), PGE surveyors Bob Buckley, Jim Tejcka, Gary Reynolds, Larry McGinnis, and Jeff Danielson, and PGE support personnel. A special thanks to the Confederated Tribes of Warm Springs, Jan Luelling, the Deschutes Club, Buck Coe, and Kenny Buck, Sr., who allowed access to the river via private property. Larry Chitwood (Deschutes National Forest) graciously offered use of field equipment as well as laboratory equipment for processing subsurface samples. This work benefited greatly from discussions with Jim O'Connor (USGS), Julia Jones (OSU), and Bob Beschta (OSU). Lisa Ganio and Barbara Marks assisted in the statistical data analysis. Diana Surgeon (North Unit Irrigation District), Larry Zakrajsek (U.S. Bureau of Reclamation), and Scott Lewis (PGE) provided historical information on dams in the Deschutes River basin. Roy Wellman (USGS) and Tom Herrett were of great help in processing ADCP data. Local offices of the Bureau of Land Management and the Oregon Department of Fish and Wildlife served as excellent resources for information and assisted with accessing some study sites.

This material is based upon work supported under a National Science Foundation Graduate Research Fellowship to Heidi Fassnacht, and by funding provided by Portland General Electric to both Heidi Fassnacht and Ellen McClure. Any opinions, findings, conclusions, or recommendations expressed in this publication are those of the authors and do not necessarily reflect the views of the National Science Foundation or Portland General Electric.

REFERENCES

Andrews, E. D., and J. M. Nankervis, Effective discharge and the design of channel-maintenance flows for gravel-bed rivers, *Natural and Anthropogenic Influences in Fluvial Geomorphology, AGU Mon., 89*, 151-164, 1995.

Aney, W. W., M. L. Montgomery, and A. B. Lichens, Lower Deschutes River, Oregon: Discharge and the fish environment, *Lower Deschutes Flow Study Final Report*, Oregon State Game Commission, Portland, Oregon, 1967.

Appel, E. P., Oregon Fishing Map: Lower Deschutes River, Frank Amato Publications, Portland, Oregon, 1986.

Chien, N., Changes in river regimes after the construction of upstream reservoirs, *Earth Surf. Proc. Landf., 10*, 143-159, 1985.

Church, M., Geomorphic response to river flow regulation: Case studies and time-scales, *Regulated Rivers: Research and Management, 11*, 3-22, 1995.

Church, M. A., D. G. McLean, and J. F. Wolcott, River bed gravels: Sampling and analysis, in *Sediment Transport in Gravel-bed Rivers*, edited by C. R. Thorne, J. C. Bathurst, and R. D. Hey, John Wiley and Sons Ltd., New York, 43-88, 1987.

Collier, M., R. H. Webb, and J. C. Schmidt, Dams and rivers: Primer on the downstream effects of dams, *U.S. Geol. Surv. Circ. 1126*, 94 pp., 1996.

DeVries, M., On the accuracy of bed-material sampling, *J. Hydraul. Res.*, *8*, 523-533, 1970.

Dietrich, W. E., J. W. Kirchner, H. Ikeda, and F. Iseya, Sediment supply and the development of the coarse surface layer in gravel-bedded rivers, *Nature*, *340*, 215-217, 1989.

Fassnacht, H., Frequency and magnitude of bedload transport downstream of the Pelton-Round Butte Dam Complex, lower Deschutes River, Oregon, M. S. thesis, Oregon State University, Corvallis, Oregon, 1998.

Ferguson, R. I., and C. Paola, Bias and precision of percentiles of bulk grain size distributions, *Earth Surf. Proc. Landf.*, *22*, 1061-1077, 1997.

Galay, V. J., R. S. Pentland, and R. A. Halliday, Degradation of the South Saskatchewan River below Gardiner Dam, *Can. J. Civ. Eng.*, *12*, 849-862, 1985.

Gannett, M. W., D. S. Morgan, and K. E. Lite, Groundwater/surface water interactions in the upper Deschutes basin, central Oregon, abstract, *EOS Trans. AGU*, *77*(46), F265, 1996.

Gilvear, D. J., and S. J. Winterbottom, Channel change and flood events since 1783 on the regulated River Tay, Scotland: Implications for flood hazard management, *Regulated Rivers: Research and Management*, *7*(3), 247-260, 1992.

Haslam, S.M., *River Plants of Western Europe: the Macrophytic Vegetation of Watercourses of the European Economic Community*, Cambridge University Press, Cambridge, U.K., 512 pp, 1987.

Hubbard, L. E., T. A. Herrett, J. E. Poole, G. P. Ruppert, and M. L. Courts, Water Resources Data, Oregon, Water Year 1996, *U.S. Geol. Surv. Water Data Rep. OR-96-1*, U.S. Geological Survey Water Resources Division, Portland, Oregon, 432 pp., 1997.

Huntington, C. W., *Deschutes River Spawning Gravel Study, Volume I, Final Report*, prepared for U.S. Department of Energy Bonneville Power Administration Division of Fish and Wildlife, Portland, Oregon, 179 pp., 1985.

Johnson, D. M., *Atlas of Oregon Lakes*, Oregon State University Press, Corvallis, Oregon, 317 pp., 1985.

Judson, S., and D. F. Ritter, Rates of regional denudation in the United States, *J. Geophys. Res.*, *69*, 3395-3401, 1964.

Junk, W. J., P. B. Bayley, and R. E. Sparks, The flood pulse concept in river-floodplain systems, in *Proceedings of the International Large River Symposium*, edited by D. P. Dodge, *Can. Spec. Publ. Fish. Aquat. Sci.*, *106*, 110-127, 1989.

Kondolf, G. M., Application of the pebble count: Notes on purpose, method, and variants, *J. Amer. Water Resour. Assoc.*, *33*, 79-87, 1997.

Krumbein, W. C., and F. J. Pettijohn, *Manual of Sedimentary Petrography*, Appleton-Century Company, New York, 549 pp., 1938.

Manga, M., Hydrology of spring-dominated streams in the Oregon Cascades, *Water Resour. Res.*, *32*, 2435-2439, 1996.

McClure, E. M., Spatial and temporal trends in bed material and channel morphology below a hydroelectric dam complex, Deschutes River, Oregon, M.S. thesis, Oregon State University, Corvallis, Oregon, 1998.

Meyer-Peter, E., and R. Mueller, Formulas for bed-load transport, in *Proceedings of the 2nd Meeting of the International Association for Hydraulic Structures Research*, 39-64, International Association for Hydraulic Research, Stockholm, 1948.

Milliman, J. D., and R. H. Meade, World-wide delivery of river sediment to oceans, *J. Geology*, *91*(1), 1-21, 1983.

Nehlsen, W., *Historical Salmon and Steelhead Runs of the Upper Deschutes River and Their Environments*, Portland General Electric, Portland, Oregon, 78 pp., 1995.

Parker, G., Surface-based bedload transport relation for gravel rivers, *J. Hydraul. Res.*, *28*(4), 417-436, 1990.

Parker, G., P. C. Klingeman, and D. G. McLean, Bedload and size distribution in paved gravel-bed streams, in *Proc. Amer. Soc. Civ. Eng. J. Hydraul. Div.*, *108*(HY4), 544-571, 1982.

Petts, G. E., Complex response of river channel morphology subsequent to reservoir construction, *Prog. Phys. Geog.*, *3*(3), 329-362, 1979.

Petts, G. E., Long-term consequences of upstream impoundment, *Environ. Cons.*, *7*(4), 325-332, 1980.

RD Instruments, *Acoustic Doppler Current Profiler Principles of Operation, A Practical Primer, 2nd Edition for Broadband ADCPs*, RD Instruments, San Diego, California, 52 pp., 1996.

Rice, S. and M. Church, Sampling surficial fluvial gravels: the precision of size distribution percentile estimates, *J. Sed. Res.*, *66*, 654-665, 1996.

Shields, I. A., Anwendung der Aehnlichkeitsmechanik und der Turbulenzforschung auf die Geschiebebewegung, *Mitteilunguen der Preussischen Versuchsanstalt f⌉r Wasserbau und Schiffbau*, translated by W. P. Ott and J. C. van Uchelen, U.S. Dept. of Agriculture Soil Conservation Service Cooperative Lab, California Institute of Technology, Pasadena, California, 36 pp., 1936.

Smelser, M. G., and J. C. Schmidt, An assessment methodology for determining historical changes in mountain streams, *Rocky Mountain Research Station Gen. Tech. Rep. RMRS-GTR-6*, U.S.D.A. Forest Service, 29 pp., 1998.

U.S. Army Corps of Engineers Hydrologic Engineering Center, HEC-RAS River Analysis System, Hydraulic Reference Manual Version 1.0, U.S. Army Corps of Engineers Hydrologic Engineering Center, California, 131 pp., 1995a.

U.S. Army Corps of Engineers Hydrologic Engineering Center, HEC-RAS River Analysis System, User' s Manual Version 1.0, U.S. Army Corps of Engineers Hydrologic Engineering Center, Davis, California, 150 pp., 1995b.

U.S. Department of Energy, *White River Falls Fish Passage Project, Tygh Valley, Oregon*, Bonneville Power Administration, Division of Fish and Wildlife Final Tech. Rep., Vol. I of III, p. 24, 1985.

U.S. Department of the Interior, Bureau of Reclamation, Reclamation Project Data (supplement), Crooked River project, U.S. Government Printing Office, Washington, D.C., 275 pp., 1966.

U.S. Department of the Interior, U.S. Geological Survey, Water Resources Division, Water Resources Data for Oregon 1965 Part I: Surface Water Records, U.S. Geological Survey Water Resources Division, Portland, Oregon, 359 pp., 1965.

U.S. Department of the Interior, U.S. Geological Survey, Water Resources Division, Description of gaging station 14-0925.00 Deschutes River near Madras, Oregon, 3 pp., 1994.

U.S. Department of the Interior Water and Power Resources Service, Water and Power Resources Service - Project Data, Deschutes River project, US Government Printing Office, 1463 pp., Denver, Colorado, 1981.

Williams, G. P., and M. G. Wolman, Downstream effects of dams on alluvial rivers, *U.S. Geol. Surv. Prof. Pap. 1286*, 83 pp., 1984.

Wolman, M. G., A method of sampling coarse river bed material, *Trans. Amer. Geophys. Un.*, *35*(6), 951-956, 1954.

Heidi Fassnacht, c/o J.E. O'Connor, U.S. Geological Survey, 10615 SE Cherry Blossom Drive, Portland, Oregon, 97216

Gordon E. Grant, U.S. Dept. of Agriculture, Pacific Northwest Research Station, Forestry Sciences Laboratory, 3200 SW Jefferson Way, Corvallis, Oregon, 97331

Peter C. Klingeman, Oregon State University, Dept. of Civil, Construction, and Environmental Engineering, 202 Apperson Hall, Corvallis, Oregon, 97331

Ellen M. McClure, Biohabitats Incorporated, 15 West Aylesbury Road, Timonium, Maryland, 21093